

U_{pper}

A_{ir}

R_{esearch}

L_{aboratory}

AD655808

THE DEVELOPMENT OF A GERDIEN CONDENSER FOR SOUNDING ROCKETS

by

David A. Burt

Contract No. AF 19(628)-4995

Project No. 7663, 5710

Task No. 766303

Work Unit No. 76630301

Scientific Report No. 8

May 1967

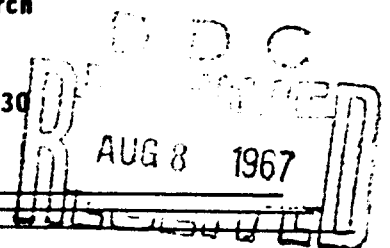
Contract Monitor: James C. Ulwick

Upper Atmosphere Physics Laboratory

Distribution of this document is unlimited. It may be released to the Clearinghouse, Department of Commerce, for sale to the general public

This research is sponsored, in part, by the Defense Atomic Support Agency, Washington, D.C. under WEB No. 07.007

Prepared for
Air Force Cambridge Research Laboratory
Office of Aerospace Research
United States Air Force
Bedford, Massachusetts 01730



RECEIVED

AUG 10 1967

CFSTI



University of Utah

Salt Lake City, Utah 84112

AFCRL-67-0343

THE DEVELOPMENT OF A GERDIEN CONDENSER
FOR SOUNDING ROCKETS

by

D. A. Burt

Upper Air Research Laboratory
University of Utah
Salt Lake City, Utah 84112

Contract No. AF 19(628)-4995
Project No. 5710, 7663
Task No. 766303
Work Unit No. 76630301

Scientific Report No. 8

May 1967

Contract Monitor: James C. Ulwick
Upper Atmosphere Physics Laboratory

Distribution of this document is unlimited. It may be released to the Clearinghouse, Department of Commerce, for sale to the general public.

This research is sponsored, in part, by the Defense Atomic Support Agency, Washington, D.C. under WEB No. 07.007.

Prepared for

Air Force Cambridge Research Laboratories
Office of Aerospace Research
United States Air Force
Bedford, Massachusetts 01730

Submitted by

Obad C. Haycock
Obad C. Haycock, Director

LIST OF CONTRIBUTORS - SCIENTISTS AND ENGINEERS

O. C. Haycock	Director
K. D. Baker	Assistant Director
A. M. Despain	Research Engineer
E. F. Pound	Research Engineer
C. D. Westlund	Research Engineer
C. L. Alley	Research Engineer
K. L. DeVries	Research Engineer

RELATED CONTRACTS AND PUBLICATIONS

AF 19(628)-447

Baker, K.D., Direct In Situ Measurements of Auroral Parameters, Scientific Report No. 4, Contract No. AF 19(628)-4995, AFCRL-66-413, UU-66-8, May 1966.

Baker, K.D., W. Pfister, and J.C. Ulwick, Charge Densities and Temperatures Measured in Active Auroras, *Space Research VII*, North Holland Publishing Co., 1966.

Burt, D.A., and K.G. Seljaas, Rocket Instrumentation for Auroral Measurements - Niros AD 7.618D and AD 7.619D, Scientific Report No. 6, Contract No. AF 19(628)-4995, October 1966.

Burt, D.A., Rocket Instrumentation for Auroral Measurements - Black Brant AC 17.604, Scientific Report No. 7, Contract No. AF 19(628)-4995, March 1967.

Despain, A.M., The Theory of Cylindrical Antenna Impedance as a Function of Plasma Frequency and Temperature, Scientific Report No. 1, Contract No. AF 19(628)-4995, AFCRL-65-480, March 1965.

Despain, A.M., Antenna Impedance in the Ionosphere, Scientific Report No. 3, Contract No. AF 19(628)-4995, AFCRL-66-412, UU-66-7, May 1966.

Howlett, L.C., Rocke: orne Auroral X-ray Instrumentation, Scientific Report No. 2, Contract No. AF 19(628)-4995, AFCRL-66-162, UU-66-4, February 1966.

Stout, D.F., A Soft Electron Spectrometer for Auroral Research, Scientific Report No. 5, Contract No. AF 19(628)-4995, AFCRL-66-694, UU-66-9, August 1966.

Ulwick, J.C., W.P. Reidy, and K.D. Baker, Direct Measurements of the Ionizing Flux in Different Types of Auroral Forms, *Space Research VII*, North Holland Publishing Co., Amsterdam, 1966.

ABSTRACT

Measurements of D-region conductivity are of extreme importance for understanding the basic, normal atmospheric processes as well as for investigating special events associated with the D-region, i.e., auroral absorptions, polar cap absorptions (PCA) and sudden ionospheric disturbances (SID). This report discusses the theory and possibilities of adapting one type of conductivity probe, the Gerdien condenser for operation on sounding rockets at supersonic and subsonic velocities. Details are presented for two systems developed for making correlating measurements during simultaneous rocket flights. The first is designed for the Black Brant II rocket (supersonic flow); and the second, employing a parachute system, is designed for the Arcas rocket (subsonic flow).

TABLE OF CONTENTS

	<u>Page</u>
Abstractiii
Table of Contents.	iv
List of Figures.	v
INTRODUCTION	1
THEORY OF OPERATION.	3
ADAPTING GERDIEN CONDENSER TO ROCKET D-REGION MEASUREMENTS . .	12
Design of D-Region Gerdien Condenser System.	17
Gerdien Condenser System for Black Brant Rocket	19
Subsonic Condenser (Arcas Parachute Deployed)	28
FLIGHT PERFORMANCE	43
CONCLUSIONS.	44
REFERENCES	45

LIST OF FIGURES

<u>Figure</u>		<u>Page</u>
1	Basic principle of operation of the Gerdien condenser.	4
2	Ideal Gerdien condenser characteristic curve for single mobility ions at constant air flow	4
3	Ideal Gerdien condenser characteristic curve for ions of three different mobilities	8
4	Theoretical Gerdien condenser characteristic curve with uniform ion velocity distribution	10
5	Gerdien condenser shock flow in the transonic region	14
6	Gerdien condenser shock flow in the supersonic region	15
7	Gerdien condenser assembly drawing	18
8	Black Brant AC 17.604 payload showing three Gerdien condensers (two side-mounted, one on erectable boom).	20
9	Black Brant Gerdien condensers	21
10	Black Brant 17.604 payload instrument mounting positions.	22
11	Gerdien condenser block diagram (Black Brant).	23
12	Gerdien condenser sweep generator (Black Brant)	24
13	Gerdien condenser sweep voltage (Black Brant).	25
14	Gerdien condenser electrometer amplifiers (Black Brant)	26
15	Gerdien condenser range switching circuitry (Black Brant)	27

LIST OF FIGURES (CONT.)

<u>Figure</u>		<u>Page</u>
16	Computed velocity curves of parachutes having varying ballistic parameters	29
17	Sketch of Scheldahl disk gap band parachute.	30
18	Packaged Scheldahl disk gap band parachute	31
19	Assembly drawing of Arcas payload.	33
20	Arcas Gerdien condenser package.	34
21	Assembled Arcas Gerdien condenser.	35
22	Sketch of Arcas Gerdien condenser payload.	36
23	Gerdien condenser block diagram (Arcas).	37
24	Gerdien condenser step generator (Arcas)	38
25	Gerdien condenser stepped voltage waveform (Arcas)	39
26	Gerdien condenser electrometer amplifier (Arcas)	40
27	Gerdien condenser range switching circuitry (Arcas).	41
28	Gerdien condenser dc-dc converter (Arcas).	42

INTRODUCTION

Experimental techniques are well developed for in situ measurements of ion and electron concentrations in the earth's atmosphere in the free molecular flow region, i.e., above approximately 90 km [Block *et al.*, 1965]. In contrast, the D-region or continuum flow region is poorly characterized since most of these experimental techniques produce measurements which are difficult or in some cases impossible to interpret because of the relatively high frequency of particle collisions. Measurements of this atmospheric region are, however, of extreme importance for understanding the basic, normal atmospheric processes as well as for investigating special events associated with the D-region, such as auroral absorption, polar cap absorption (PCA), and sudden ionospheric disturbances (SID). The increased collisional frequency at the lower altitudes suggests that the determination of atmospheric conductivity should be the basic technique for making the needed measurements. A conductivity probe which appears adaptable to rockets is a device developed by H. Gerdien [1905] consisting of two, concentric cylinders through which air flows. The atmospheric conductivity is obtained by measuring the current flow between the cylinders. Historically, many of these devices (which were termed Gerdien condensers) were placed on various vehicles (principally sailing ships) and mounted at permanent sites over the globe to make conductivity measurements at the surface of the earth [Kidson, 1910].

With the advent of the sounding rocket and direct, in situ, atmospheric measurements, it was desirable to extend the range of the Gerdien

condenser into the D-region for determination of electron densities, ion densities and ion species.

The major problem associated with flying the Gerdien condenser on a rocket is the speed at which the rocket travels in the region. It is possible that too great a speed could cause ionization which would invalidate all attempted measurements; and at transonic speeds, it is difficult to determine the mass rate of air flow through the condenser. The theory of Gerdien condenser operation, a discussion of problems particular to rocket mounted condensers, and the description of a system developed for rocket measurements in the D-region are contained in this report.

THEORY OF OPERATION

The basic principle of operation for the Gerdien condenser is the measurement of the current to the rocket due to a sweep voltage applied to a concentric, cylindrical capacitor through which the air is flowing as shown in Figure 1. With the voltage polarity shown, positive ions will be accelerated toward and collected on the center cylinder while negative charges will be collected on the outer cylinder. With the voltage and current referenced to the rocket body, it is possible for the negative and positive currents to be different. If a plasma having positive ions of a single species enters the cylinder at a constant velocity directed parallel to the cylinder axis, the current as a function of the applied voltage will be as shown in the ideal characteristic curve of Figure 2. Assuming that many collisions occur within the condenser, the voltage-current relationship is linear until a voltage is reached at which all charged particles are collected. This assumption of a large number of collisions limits the basic operation of the condenser to an altitude at which the mean, free path of any particle is much less than the distance between the outer and inner cylinders.

In the saturated region, the current for a plasma with a singly charged ion species will be

$$I_s = n_i e v A \quad (1)$$

where

I_s = Gerdien condenser saturation current

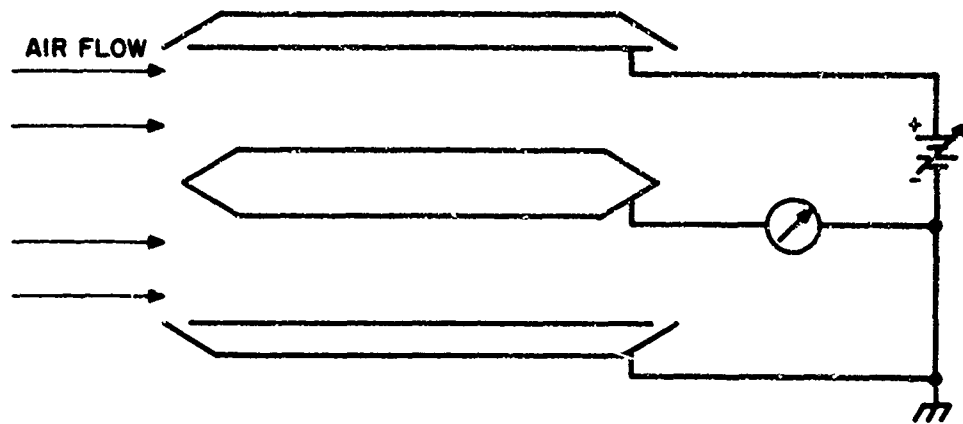


Fig. 1. Basic principle of operation of the Gerdien condenser.

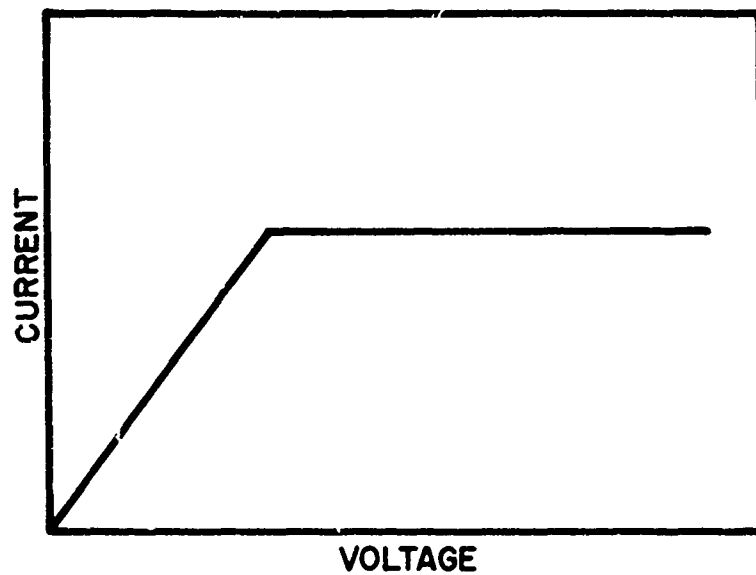


Fig. 2. Ideal Gerdien condenser characteristic curve for single mobility ions at constant air flow.

A = aperture area of Gerdien condenser

v = initial velocity of air entering condenser

e = unit charge 1.6×10^{-19} coulombs

n_i = number of ions per unit volume of species i

This expression indicates that the ion density n_i can be found from the instrument geometry, the air entry velocity, and the measured ion saturation current. The second region of interest is the linear portion of characteristic curves prior to saturation. The radial current density in the condenser is given by

$$J = n_i e \bar{v}_i \quad (2)$$

where

J = current density

\bar{v}_i = average drift velocity of particles due to applied electric field

Dividing both sides of (2) by the electric field E gives the conductivity σ_i

$$\sigma_i = n_i e \frac{\bar{v}_i}{E} \quad (3)$$

If the term \bar{v}_i/E defined as the ion mobility is designated by μ_i , then

$$\sigma_i = n_i e \mu_i \quad (4)$$

If field-fringing end effects are neglected in the condenser, the conductance of the cylinder G_i due to ions n_i (slope of the characteristic curve of Figure 2) will be

$$G_i = \frac{2\pi\sigma_i L}{\ln r_2/r_1} = \frac{2\pi n_i e \mu_i L}{\ln r_2/r_1} \quad (5)$$

where

L = length of condenser

r_2 = inside radius of outer cylinder

r_1 = outside radius of inner cylinder

Equation (5) shows that the slope of the current-voltage curve of the condenser will give a determination of both the ion conductivity and mobility.

This expression may be rewritten as

$$G_i = n_i e \mu_i C / \epsilon_0 \quad (6)$$

where

C = capacitance of cylinder

ϵ_0 = permittivity of free space

Swann has shown that if the actual, measured capacitance of the cylinder is used instead of the calculated capacitance, the results will be more accurate [Swann, 1914].

The derivation of (6) does not consider the effects of air velocity; however, a consideration of air velocity effect in the non-saturated region does indicate that (6) should be independent of air velocity. This is an important concept and will be discussed later.

In actual practice, air will be a multiple-constituent gas; thus all ions will not have the same mobility. Each ion species will have its own characteristic, and the total current will be the composite of that due to each ion species. A theoretical curve is shown in Figure 3, consisting of straight line segments for three single mobility ions. The voltage-current relationship will still remain linear until all the ions having the highest mobility are collected. At this point, the slope of the curve will change due to saturation of that component of ion current. As the voltage is further increased, a break will occur in the curve at the point of total collection of each ion species of lower mobility until all ions are collected. This saturation current will be given by

$$i_s = \sum_i n_i e v_i = n_t e v_A \quad (7)$$

where n_t = ion density of all species.

If higher order ions, i.e., doubly or triply ionized atoms, exist in significant quantities, the current would be modified according to the higher ion charge; however, it appears that the number of singly ionized positive ions is much greater than the higher ionized particles [Narcisi, 1965]. The total conductance is the summation of the conductance due to each ion component of the plasma

$$G = \sum_i n_i e \mu_i C / \epsilon_0 = \sum_i G_i \quad (8)$$

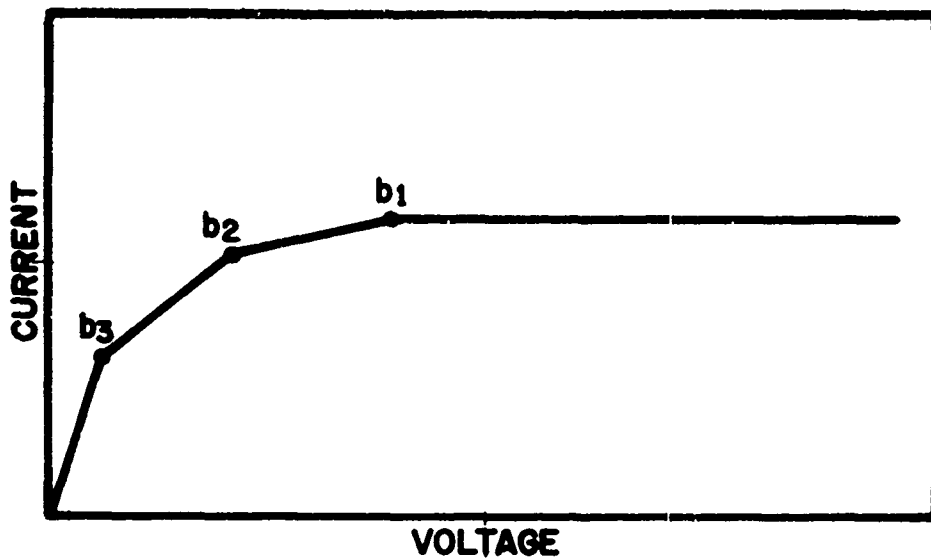


Fig. 3. Ideal Gerdien condenser characteristic curve for ions of three different mobilities.

In (8), there are two unknowns, the mobility and the number density of each species. Equation (7) gives the total positive ion density from the saturation current (point b_1 of Figure 3). With this value of n_t , the initial slope will then give the total ion mobility (8).

Additional information on individual ion mobilities and densities can be derived from this curve by further analysis. The saturation point of the lowest mobility ion is b_1 , b_2 the next highest, and b_3 the highest mobility. The slope of the line from b_2 to b_1 (G_1) times the voltage at b_1 is the saturation current for the lowest mobility particle, the slope of b_3 to b_2 minus the slope of b_2 to b_1 times voltage at b_2 is the saturation current of the next highest particle. Accordingly,

$$I_1 \text{ sat} = v_1 \left(\frac{I_1 - I_2}{v_1 - v_2} \right) = v_1 G_1 \quad (9)$$

$$I_2 \text{ sat} = v_2 \left(\frac{I_2 - I_3}{v_2 - v_3} - G_1 \right) = v_2 G_2 \quad (10)$$

$$I_3 \text{ sat} = v_3 \left(\frac{I_3}{v_3} - G_2 - G_1 \right) = v_3 G_3 \quad (11)$$

where $I_1 \text{ sat}, I_2 \text{ sat}, I_3 \text{ sat}$ = saturation current resulting from each different mobility ion

G_1, G_2, G_3 = conductance due to each ion species

Once the saturation currents and ion conductivities are known, the ion number densities follow from (1) and the ion mobilities from (6) for each constituent.

In actual measurements, due to thermal agitation and initial velocities not being uniform and not being directed entirely parallel to the condenser, the characteristic curve will not break as sharply as shown in Figure 3. This, coupled with the fact that a large number of straight-line segments are hard to distinguish from a curve, makes it difficult to identify the break point of each species. The theoretical characteristic curve will appear as shown in Figure 4.

It is more convenient to write equations of the type (9), (10), and (11)

$$I_n \text{ sat} = v_n \left[\frac{di}{dv} \Big|_{v_n} - \frac{di}{dv} \Big|_{v_{n-1}} \right] \quad (12)$$

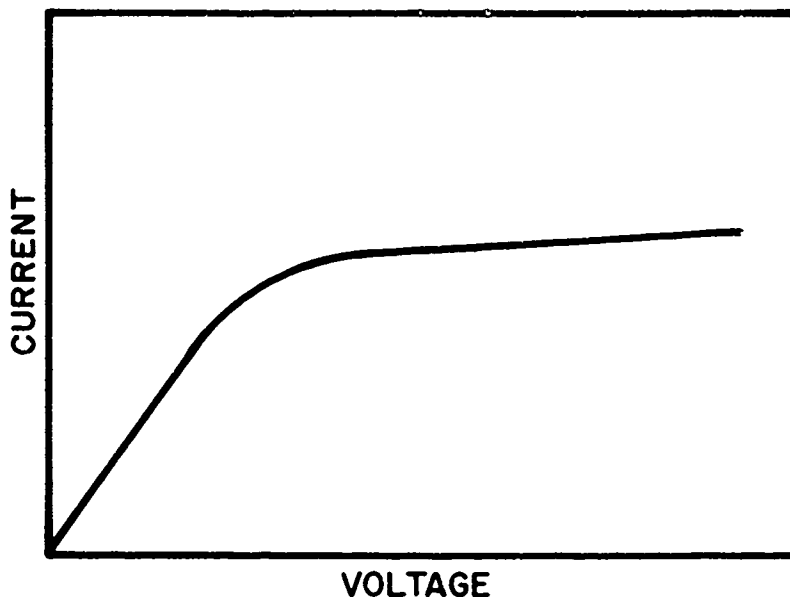


Fig. 4. Theoretical Gerdien condenser characteristic curve with uniform ion velocity distribution.

The term in the brackets can then be defined as G_1 . From (12), G_1 is proportional to the second derivative of the current with respect to the voltage. This would indicate a simple solution to determine mobility by applying a proportionality constant to the second derivative. This would, of course, require extremely smooth data which is unlikely. It should be possible to obtain meaningful information from any reasonable data by judicious smoothing and by applying (12) to a computer program.

The preceding equations were written for positive ions; however, if the polarity of the sweep generator in Figure 1 is reversed, the center electrode would collect the negative charges. The same equations would hold then for both negative ion and free electron measure-

ments; although these particle mobilities will cover a larger range.

Since the electron binding energy of the negative ion is a few ev, the necessary high voltage gradient in the condenser may cause detachment unless the condenser has a large length to radius ratio. However, at supersonic speeds, lengthening the condenser could cause problems due to increased turbulence inside the condenser.

ADAPTING GERDIEN CONDENSER TO ROCKET D-REGION MEASUREMENTS

As noted, the major problem associated with using the Gerdien condenser on a rocket is the difficulty in interpreting the measurements at rocket speeds. Two approaches for making these data more amenable to solution are proposed. One involves holding the device to subsonic speeds as Pedersen has done by the use of a parachute on reentry [Pedersen, 1965]. The second entails the development of a condenser which would work at supersonic speeds.

A parachute for this application must be of special design for high altitude operation. It must remain open in the sparse atmosphere and be stable, i.e., have a small coning angle. Depending upon the height of ejection, it may have to function at supersonic speeds for the first part of the flight. The size of the payload must be small, thereby limiting the payload to essentially one experiment which precludes the possibility of comparing different experiments on the same payload by making multiple simultaneous measurements.

The problems associated with the parachute payload are eliminated by operating the Gerdien condenser at supersonic speeds on the side of a rocket. This, however, introduces new problems concerned with what happens to the measurements at these speeds and involves the following considerations:

1. What is the actual flow through the condenser at transonic and supersonic speeds?
2. Can the unit be made to withstand the aerodynamic heating and stresses?

3. How much of an enhancement to ionization is there in the shock?

4. Will the Gerdien condenser protrusions cause any instability in the rocket?

It was decided at this time to try both the subsonic and the supersonic methods simultaneously, i.e., to have a condenser descend on a parachute and at the same time have an identical one ascending on a rocket. A Black Brant rocket was chosen as the vehicle for the supersonic flight as its payload was designed for multiple experiments which would give cross calibration to other experiments. A sidewinder Arcas (hereafter referred to only as Arcas) was selected as the vehicle to carry the subsonic parachute payload aloft.

Below sonic speeds, the relative velocity of the plasma intersected by the aperture of the condenser will increase as it passes through the condenser. If the gas reaches sonic velocity in the condenser, choking will occur and an unattached shock wave will form as shown in Figure 5. As can be seen, some of the air which would normally flow through the condenser is diverted, having the effect of reducing the aperture of the condenser. At the present time, the volume rate of flow through this region where choking occurs cannot be accurately determined. As the speed of the air through the condenser is increased further, the shock wave will move closer to the condenser until the following two conditions are met:

1. The speed must increase until the area ratio of the inner and outer cylinders is such that flow will slow down to where it is equal to or greater than Mach 1.

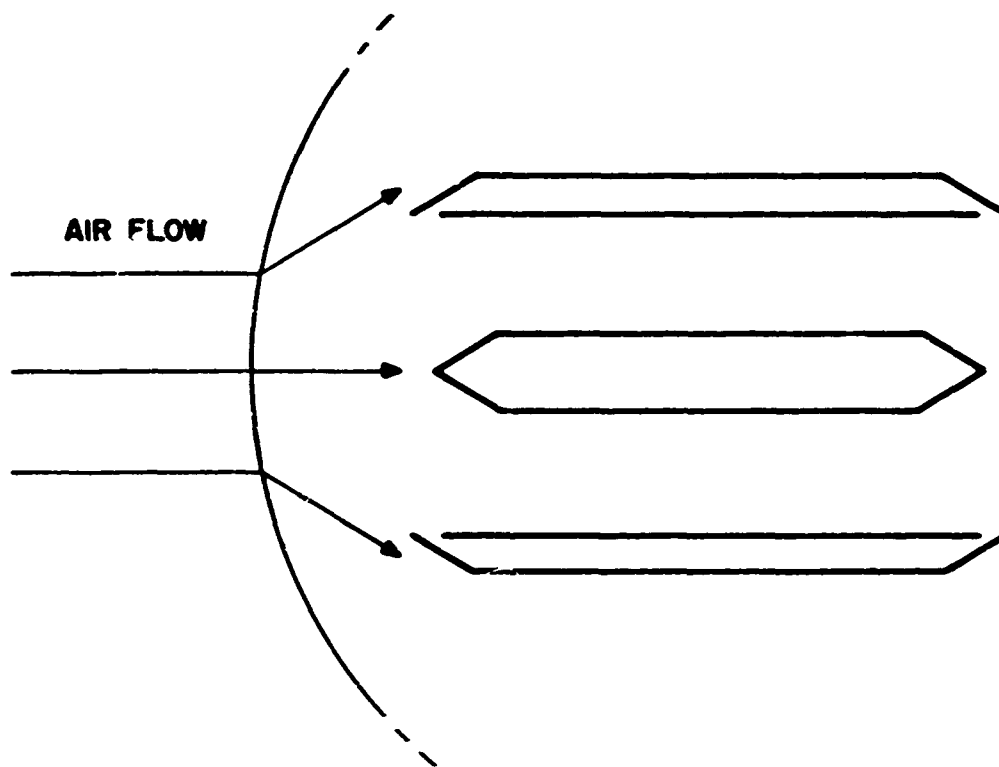


Fig. 5. Gerdien condenser shock flow in the transonic region.

2. The shock created by the center cylinder is swallowed by the condenser and the shock of the outer cylinder becomes attached. When this occurs, the air flow will be as shown in Figure 6.

As shown in (7), the conductivity in the nonsaturated region is independent of velocity. For high velocities, however, temperature, pressure, and density were omitted in the derivation of this equation. Since the condenser is a converging throat and since there is a shock flow, these parameters must vary from the ambient as it flows through the cylinder. The value of these variations must be ascertained so that all readings can be referred back to the ambient. If the velocity is known, air flow tables [Lleymann, 1957] can be used to approximate these changes.

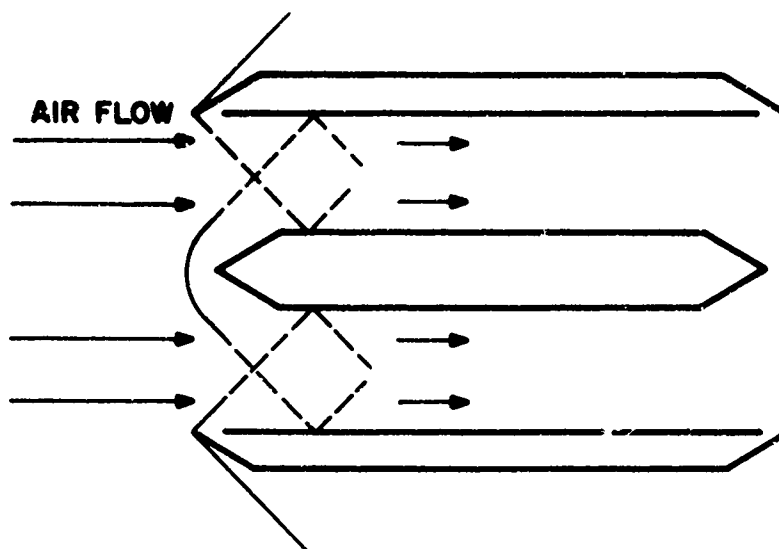


Fig. 6. Gerdien condenser shock flow in the supersonic region.

There was considerable concern as to whether there would be creation of new ions as the air flows through the bow shock. As the air flows through the shock wave, the pressure (P), the temperature (T), and the density (ρ) suffer discontinuous jumps. Shock strength calculations for a Black Brant rocket are given in Table 1. Only a normal shock is considered since this will produce the maximum change.

In Table 1, subscript 1 refers to the conditions prior to the shock, and subscript 2 refers to conditions behind the shock.

By using the maximum temperature of 813°K and assuming normal reversible reactions as in equations developed by *Saha and Srivastava* [1958], the production of new ions by the shock wave will be much less than the resolution of the instrument. If a detachment potential of a

TABLE 1. Calculated Normal Shock Strength

Altitude (km)	Mach N	T_2/T_1	T_1 (°K)	T_2 (°K)	P_2/P_1	P_1 (Torr)	ρ_2/ρ_1	ρ_1	Kg/m ³
50	3.23	3.0	271	813	11.8	.598	4.05	1.02×10^{-3}	
55	3.09	2.8	266	744	11.0	.320	3.95	5.6×10^{-4}	
60	3.04	2.7	256	691	10.6	.156	3.90	2.85×10^{-4}	
65	2.995	2.7	239	645	10.4	.078	3.85	1.53×10^{-4}	
70	2.969	2.65	220	583	10.1	.037	3.82	7.88×10^{-5}	
75	2.952	2.62	200	524	10.0	.016	3.80	3.80×10^{-5}	

few ev is used for negative ions, the shock detachment for negative ions will also be negligible.

It was shown in the original condensers that air turbulence inside the condenser had no affect on the measurements [Swann, 1914]. This, however, was done for low velocities of air flow where the average thermal velocity of a particle was much greater than any turbulence that could be created. At supersonic speeds this will not be the case since the thermal velocity at the altitudes specified is on the order of the speed of sound. It is conceivable that turbulence at supersonic speeds could actually carry a particle in such a direction as to oppose the applied electric field. For this reason it is important that the condenser be designed to allow as laminar an air flow as possible. However, it is highly desirable that wind tunnel tests be used to determine the actual flow.

Design of D-Region Gerdien Condenser System

The following parameters were considered in devising an optimum mechanical design for a rocket Gerdien condenser.

1. The requirement of cross calibration between the subsonic and the supersonic condensers made identical condensers desirable.
2. To prevent additional ionization of the air due to the condenser, the cylinder ratio of length to diameter should be large enough that high voltage gradients are not necessary to collect all the particles.
3. The radius of the condenser should be large compared to the mean free path of particles being measured.
4. The unit must physically fit the rockets and be able to survive the rocket environment.
5. The condenser should not disturb the rocket aerodynamics appreciably for all flight speeds.

The condenser was designed with radii of 9.4 and 1.25 cm for the outer and inner cylinder, respectively, and a length of 17.5 cm with a measured capacitance of 11 pf. An assembly drawing of the condenser is shown in Figure 7.

Due to the limited size of the Arcas rocket, it was found that Item Nos. 1 and 4 were the most critical for determining the outside physical dimensions of the condenser. The size determined does, however, fit all other requirements with the exception that the length to diameter ratio is low enough that electron detachment could take

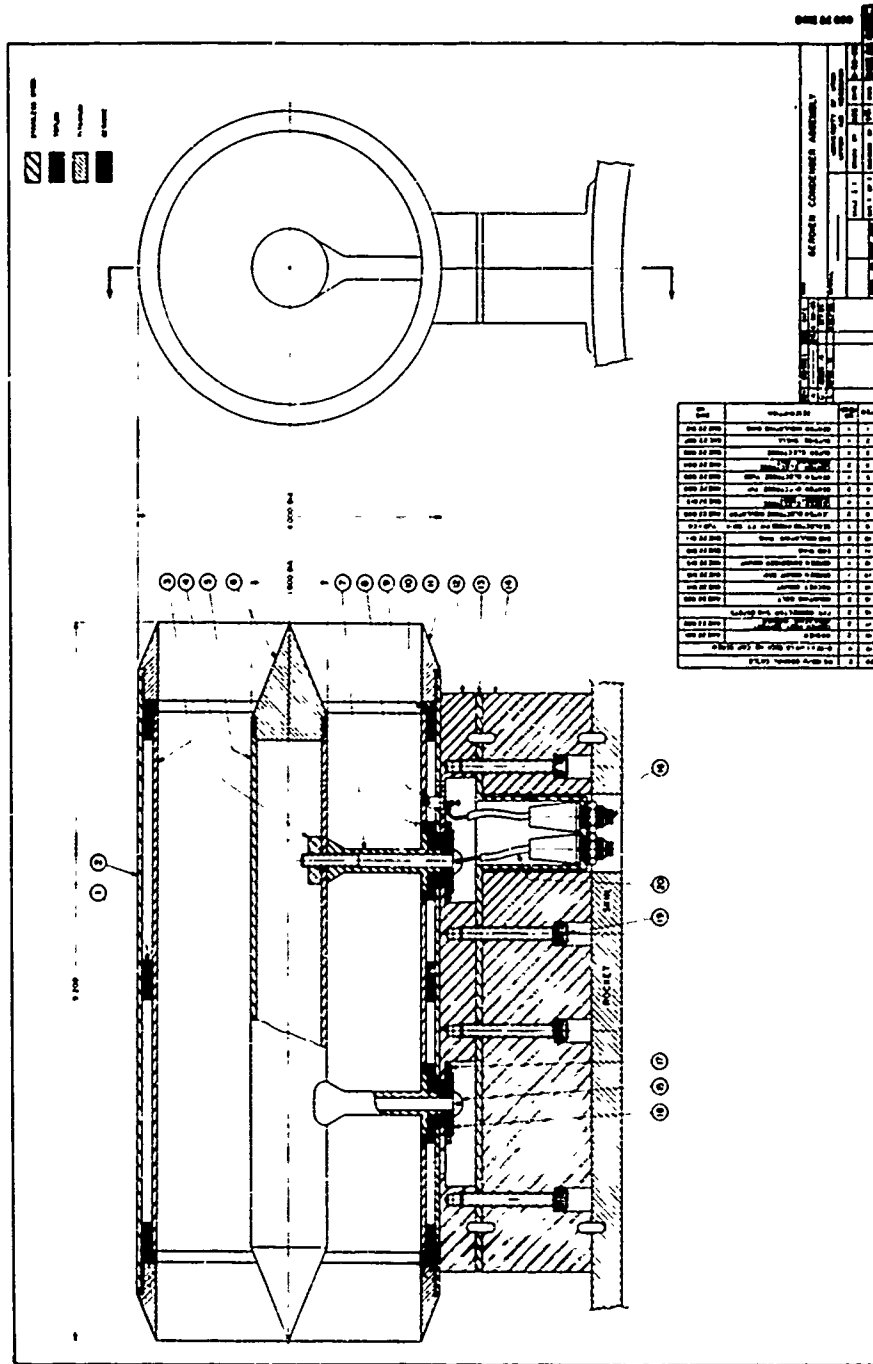


Fig. 7. Gerdien condenser assembly drawing.

place when trying to measure negative ions. At altitudes of 70 to 75 km, it is also possible to ionize some neutral particles.

The altitude at which the condenser ceases to operate as a conductivity probe is determined by the ratio of the radius of the condenser to the ion mean free path. If a minimum ratio of 10 is taken as a limit, the present radius would allow a maximum altitude of 78 km. Any further increase in the condenser diameter of practical dimensions would result in very little altitude increase.

The point at which choking will occur as determined from airflow tables [Llepmann, 1957] is approximately Mach 0.7. The point at which choking should cease is Mach 1.35. However, due to the turning angle of both the outer and inner cylinder, the shock will not become attached until Mach 1.85.

GERDIEN CONDENSER SYSTEM FOR BLACK BRANT ROCKET

Three condensers were built to fly at supersonic speeds. Two of these condensers were mounted permanently on the side of the Black Brant rocket and were made from stainless steel with titanium end pieces to withstand heating. The third condenser was made of magnesium and mounted on a boom which was to extend about 1 meter normal to the rocket axis when the rocket reached 50 km (see Figure 8). A photograph of the finished Black Brant condensers is shown in Figure 9.

The mounting positions on the rocket are shown in Figure 10. One of the side-mounted condensers was driven to collect electrons and negative ions. The other side-mounted unit and the one on the boom were driven to collect positive ions.

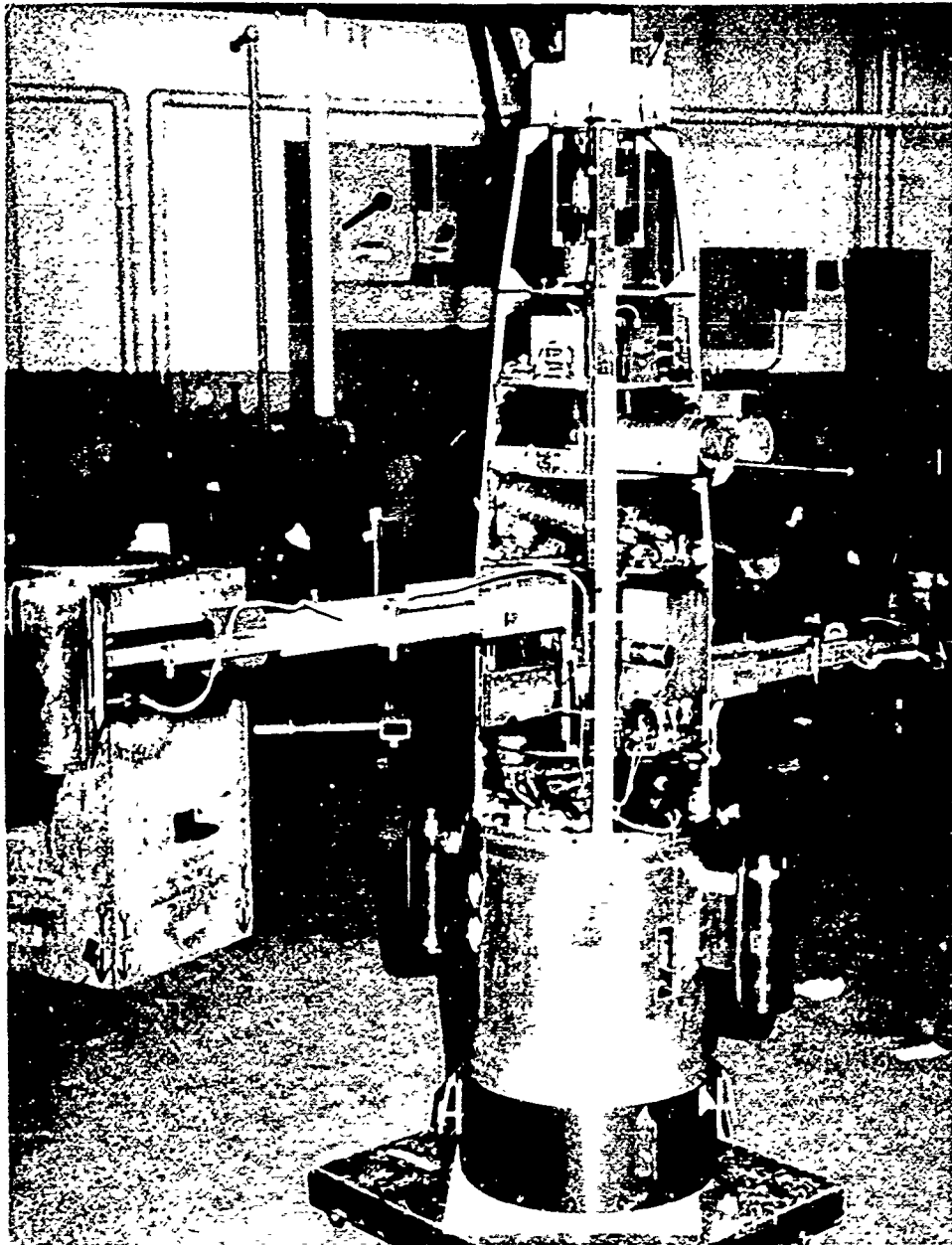


Fig. 8. Black Brant AC 17.604 payload showing three Gerdien condensers (two side-mounted, one on erectable boom).

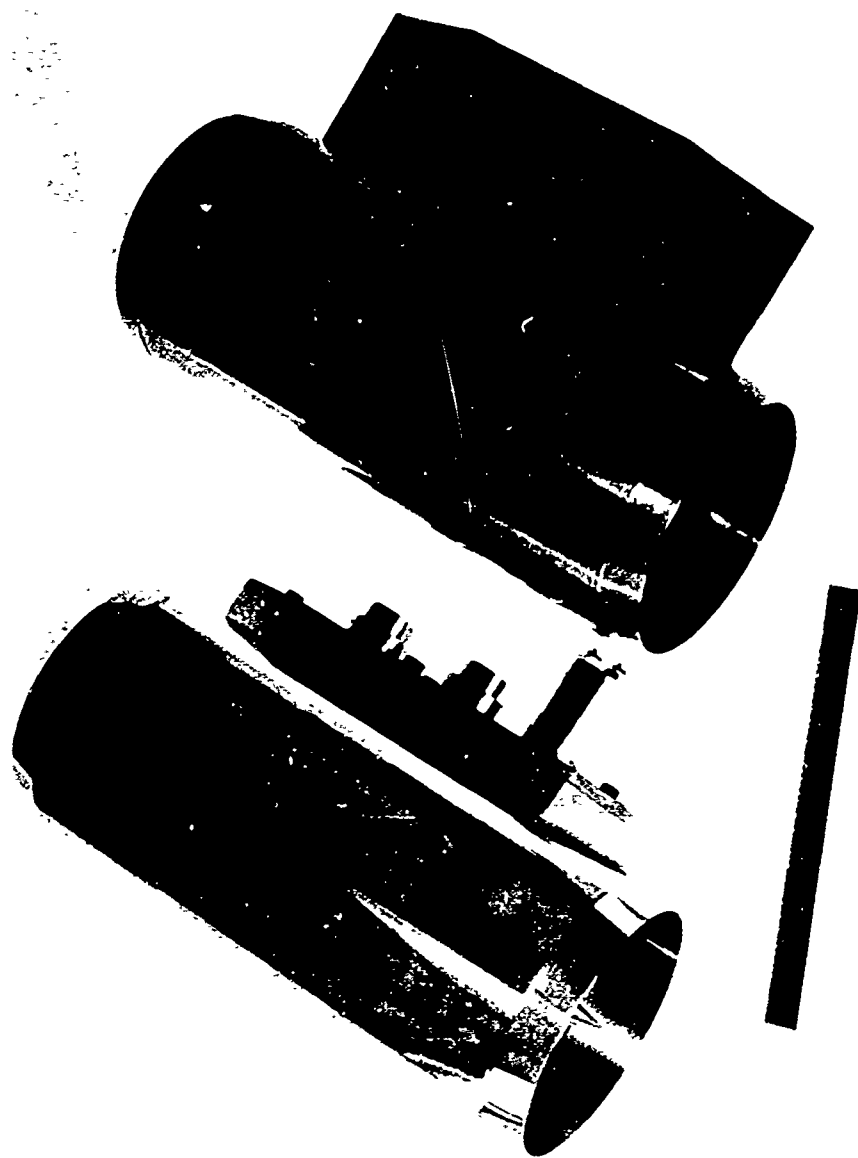


Fig. 9. Black Brant Gerdien condensers.

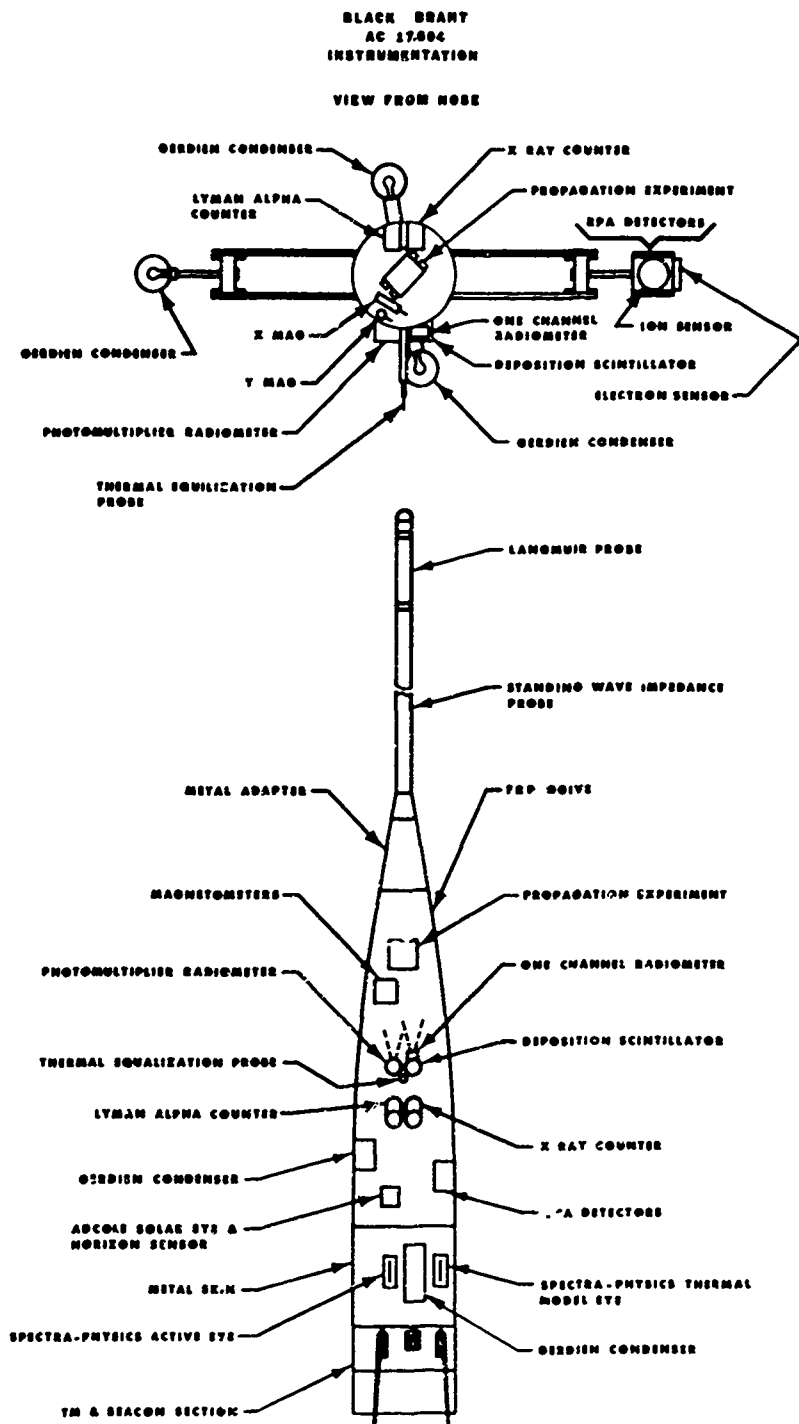


Fig. 10. Black Brant 17.604 payload instrument mounting positions.

A block diagram of the electronics for one condenser is shown in Figure 11. The sawtooth of the sweep generator produces a sweep voltage which is applied to the outer cylinder of the condenser. The center electrode current is applied to the amplifier which has three gain ranges, each differing by a factor of ten for the three successive sweeps.

The sweep generator (Figure 12) is basically a relaxation oscillator followed by an integrator, amplifier, and phase inverter producing the waveform shown in Figure 13. This circuit also provides an opposite polarity sweep which is fed back through a neutralizing capacitor to cancel the displacement current in the condenser.

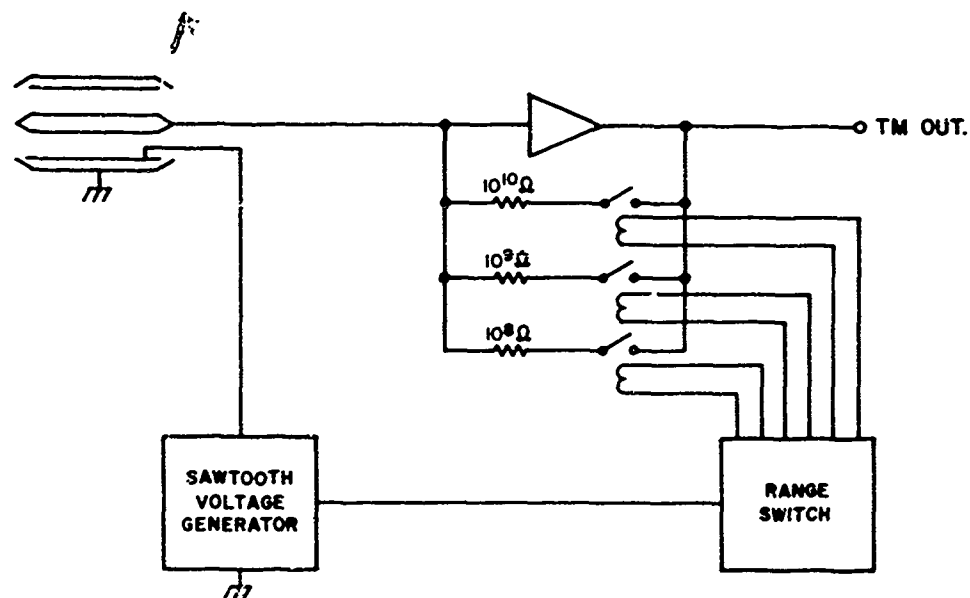


Fig. 11. Gerdien condenser block diagram (Black Brant).

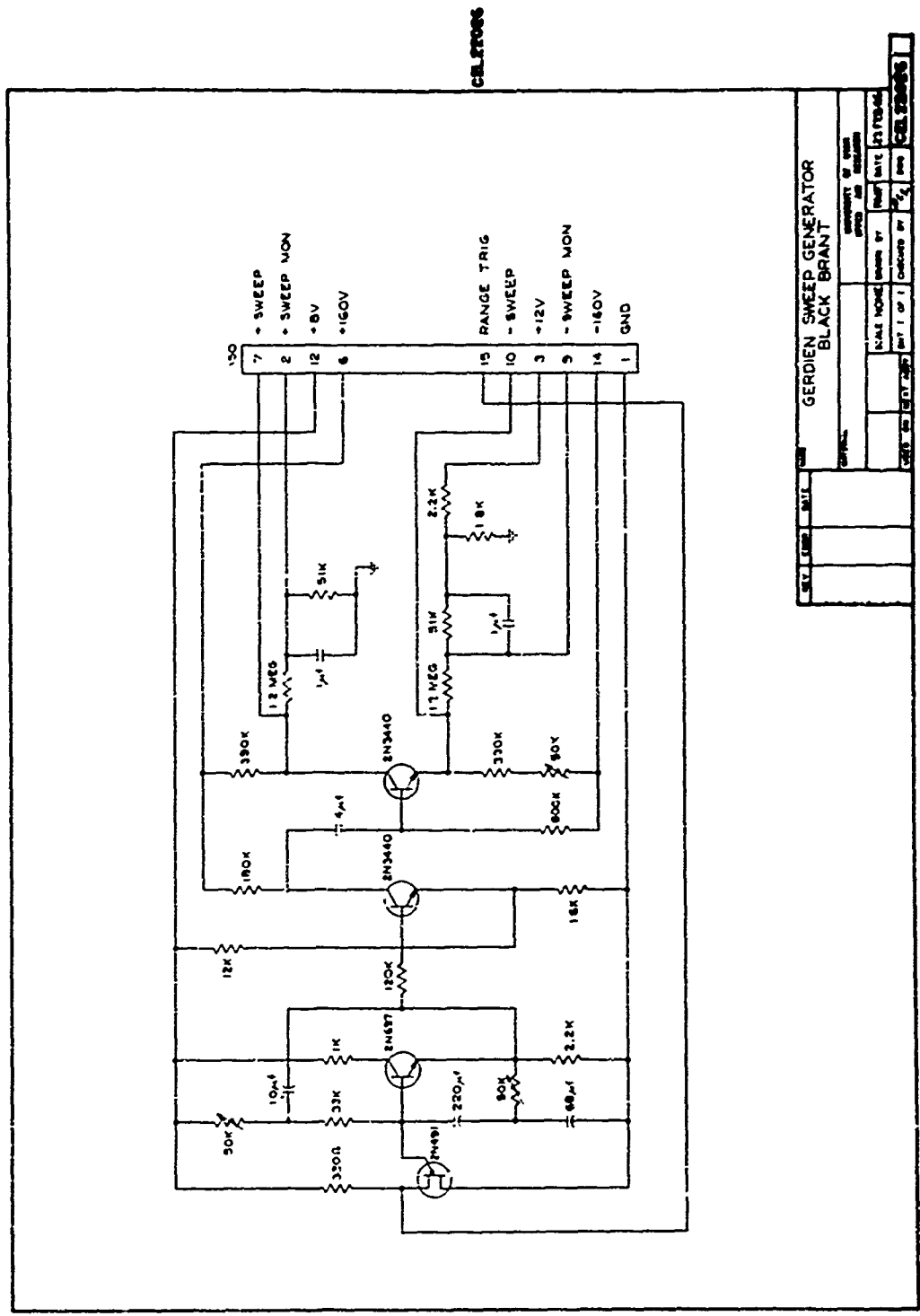


Fig. 12. Gerdien condenser sweep generator (Black Brant).

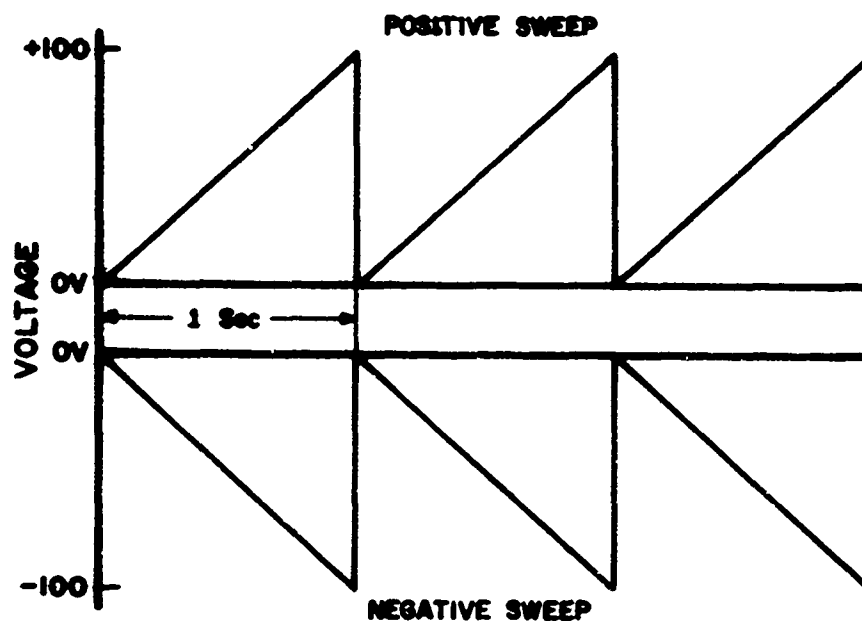


Fig. 13. Gerdien condenser sweep voltage (Black Brant).

The multigain amplifier (Figure 14) utilizes an MOS transistor for high input impedance. The amplifier gain is determined by the feedback resistors which are selected by a high impedance reed relay. The reed relays are controlled by the range switch (Figure 15) which is triggered by the retrace of the sweep generator.

The amplifier gain was set to measure ion densities from about 20 to 2×10^4 ions/cm³ in the following manner. For a maximum velocity of 3.5×10^3 ft/sec, the maximum current would be 5×10^{-8} amps for a density of 10^4 cm⁻³. Accordingly, the least sensitive range was set with a 10^8 ohm feedback resistance to give a maximum current of 5×10^{-8} amps. The highest gain range with the 10^{10} ohm feedback resistor then had a sensitivity of about 20 cm⁻³.

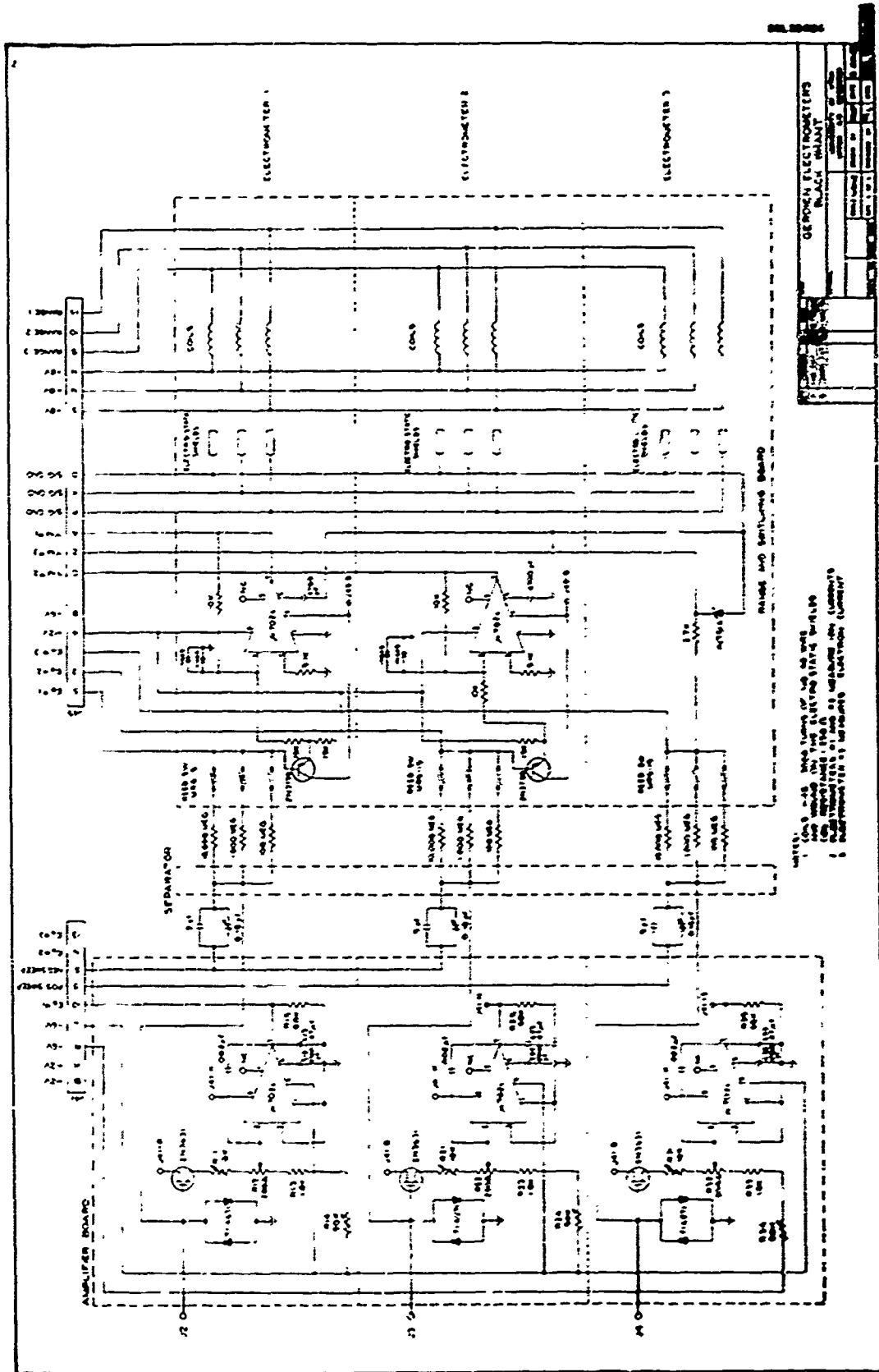
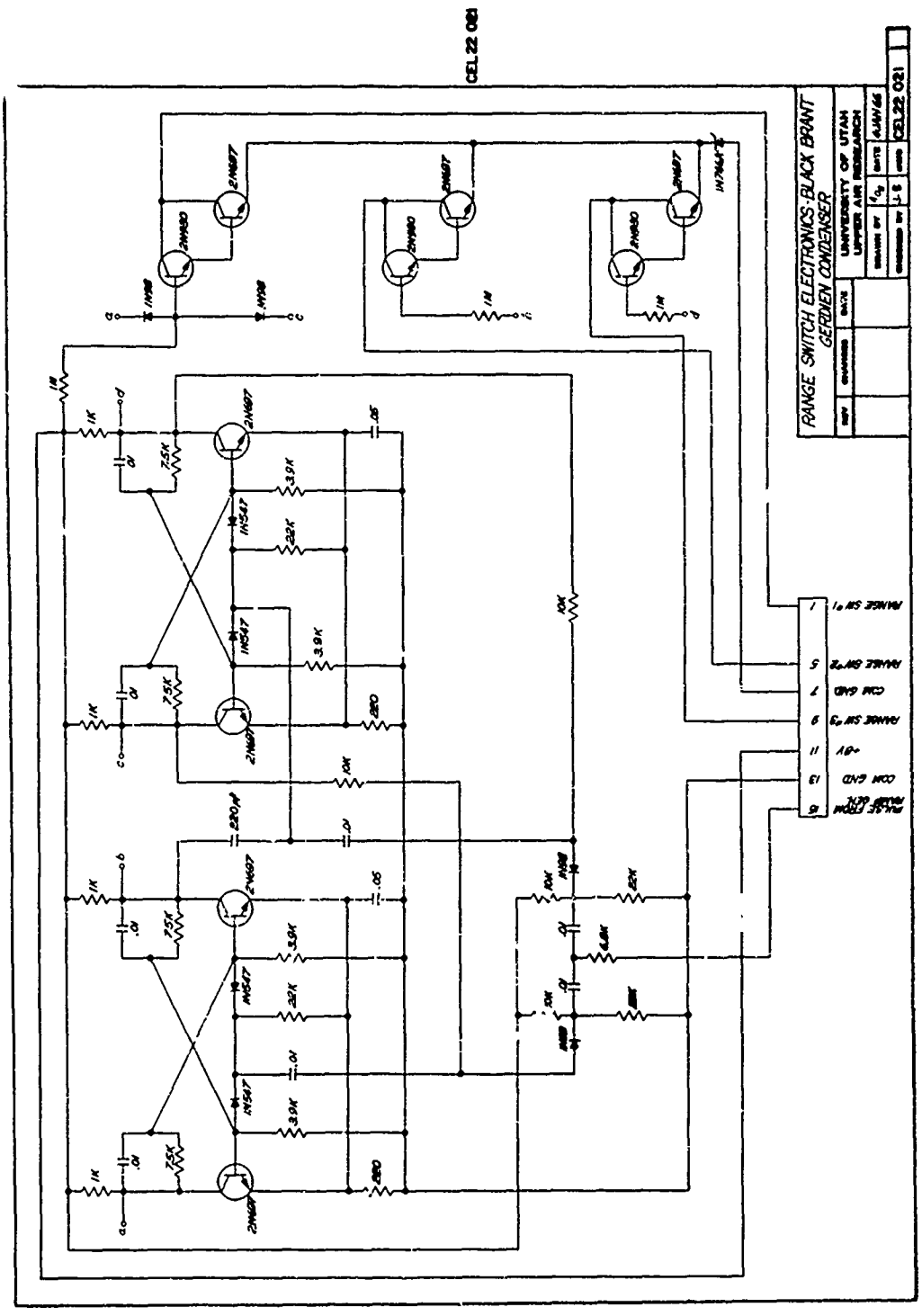


Fig. 14. Gerdien condenser electrometer amplifiers (Black Brant).



RANGE SWITCH ELECTRONICS-BLACK BRANT	
DATE	APR 1966
DESIGNED BY	CEL 22 021
CHECKED BY	
APPROVED BY	
UNIVERSITY OF UTAH	
UPPER MERIT AIR RESEARCH	
PROJECT NO.	CEL 22 021
REVISION NO.	1

Fig. 15. Gerdien condenser range switching circuitry (Black Brant).

Based on the assumption that the conductivity of the air at sea level would be the lowest conductivity encountered, the maximum sweep voltage was set at 100 volts in order to collect all the charge flowing through the condenser. The output of the amplifier for each of the three Gerdien condensers was applied to a telemetry channel with two additional telemetry channels monitoring the sweep voltages.

SUBSONIC CONDENSER (ARCAS PARACHUTE DEPLOYED)

Since the Arcas rocket was designed to eject a payload on a parachute, it was decided to use this vehicle to carry the condenser. The choice of the correct parachute, however, was more difficult. There is considerable work being done on high altitude, high speed parachutes at this time [Morrow, 1960; Whitlock and Morrow, 1964]. In a rarefied atmosphere, parachutes have trouble opening and can be unstable depending on their height of ejection. In addition, they may have to work at supersonic speeds for part of the flight.

In order to know the mass rate of air flow through the condenser, it is necessary to know its angle of attack. If the parachute is oscillating, a radar track can be used to determine its velocity, but it is very difficult to determine the condenser angle of attack at any given time.

Figure 16 shows computer curves for the velocity of parachutes with different ballistic parameters ($W/C_D S$ where W = weight, C_D = drag coefficient, S = projected frontal area), assuming that each parachute was dropped at 300,000 feet. While the altitude at which the parachute

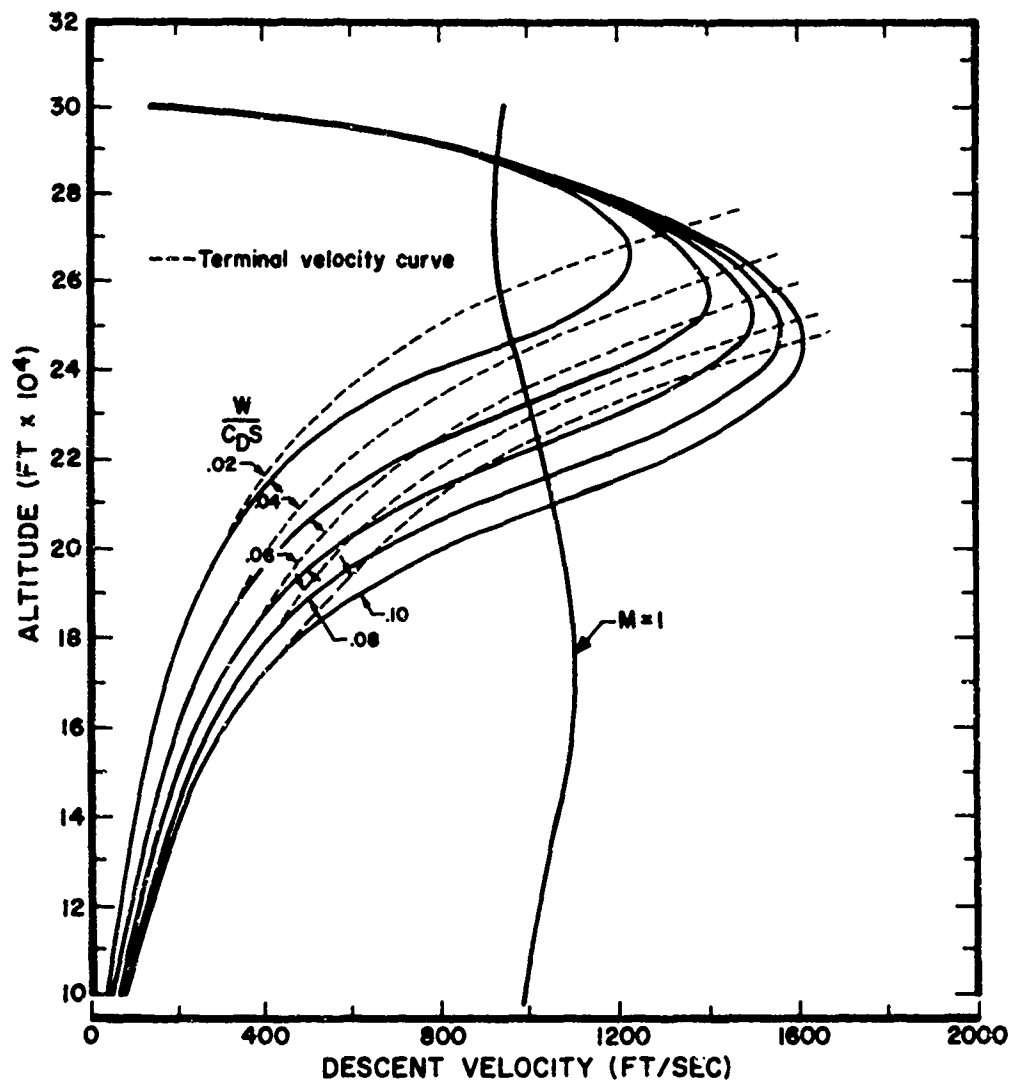


Fig. 16. Computed velocity curves of parachutes having varying ballistic parameters. (Ejection altitude 300,000 feet; Mach 1 velocity is shown as $M = 1$.) [H.N. Murrow, personal communication 1965].

starts to travel at subsonic speeds is slightly dependent on the ballistic parameters, the altitude at which it occurs is also in the same area that the Gerdien condenser begins to act as a conductivity probe. In order to have the parachute open and function at the highest possible altitude, it may be necessary to have a parachute that is capable of working at supersonic speeds. The distance above the point at which the parachute operates subsonically should be held to a minimum to shorten the time of supersonic speed.

The parachute which best seemed to fill the requirements was a Mylar disk gap band parachute built by Scheldahl Company and is shown in the drawing of Figure 17 and in the packaged form in Figure 18.

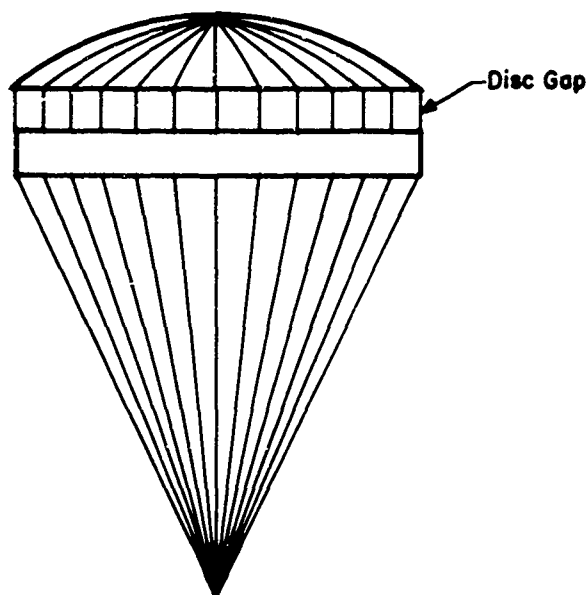


Fig. 17. Sketch of Scheldahl disk gap band parachute.

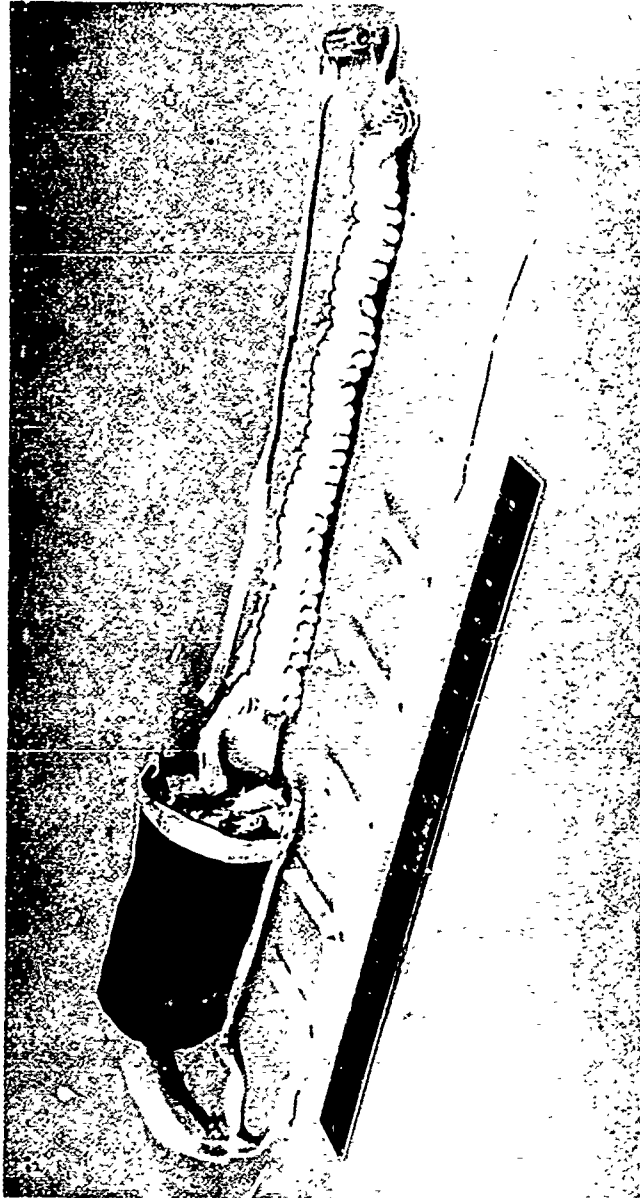


Fig. 18. Packaged Scheidahl disk gap band parachute.

The inflation of this parachute is accomplished by a torus around the band at the maximum diameter of the parachute. Blotters containing water are sealed inside the torus so that at low pressures the water evaporates and inflates the torus. Studies have shown that this configuration has good stability at high altitudes and speeds (H.N. Murrow, personal communication, 1965).

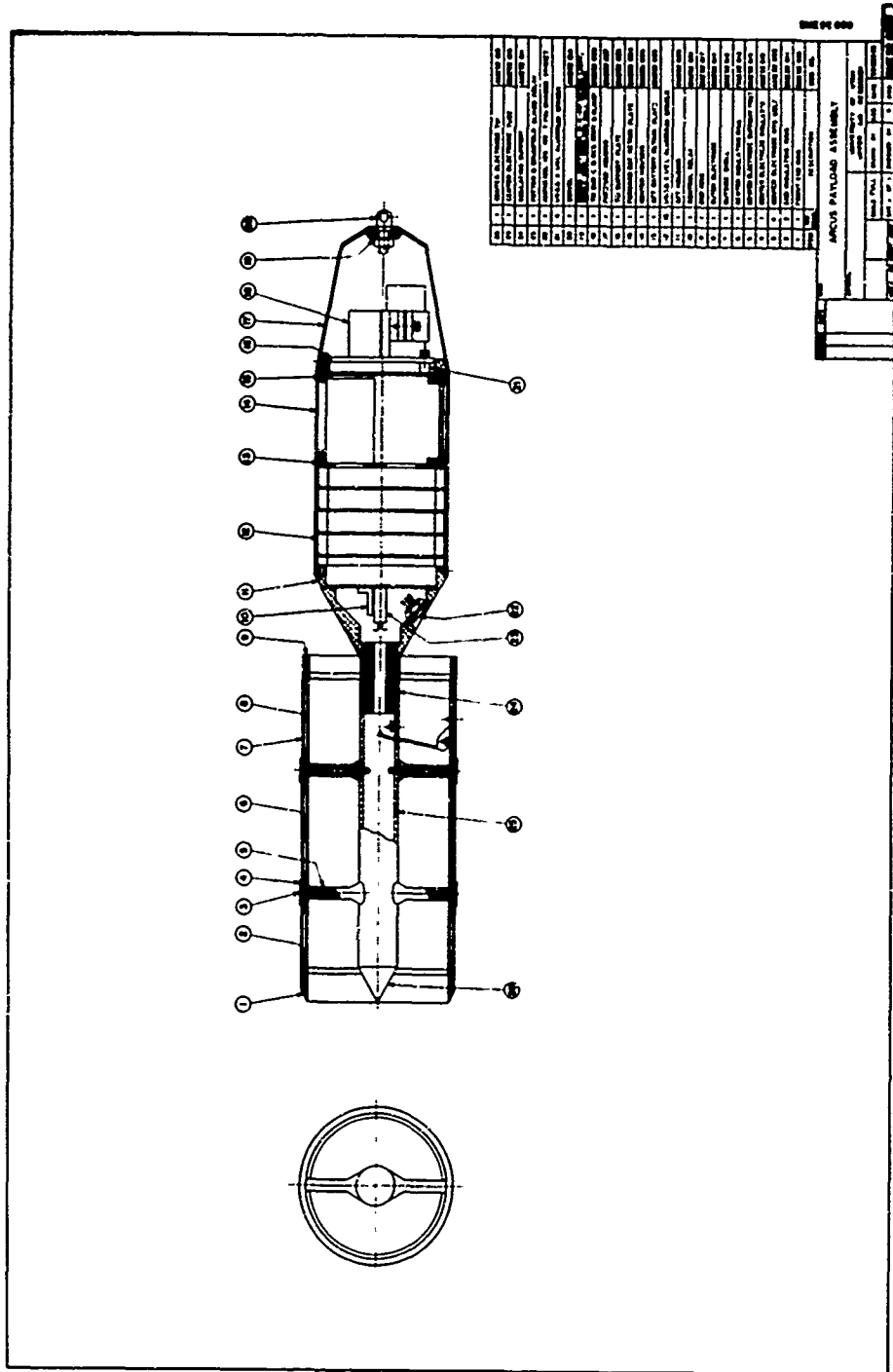
Two Arcas payloads were constructed as shown in the assembly drawing of Figure 19 and in the payload photographs of Figures 20 and 21. This configuration requires an 11-inch extension on the Arcas nosecone and is packaged in the rocket as shown in Figure 22.

The gas generator was ignited and ejected the payload at 100 seconds after launch. A length of 1/16 inch piano wire was used as a connection from the condenser to the parachute to minimize the possibility of the payload becoming entangled as the payload rotates to its correct attitude.

A block diagram of the electronics for the Arcas package is shown in Figure 23. The condenser electronics was identical to the Black Brant unit with the exception that a step generator was substituted for the sweep generator. The output of the amplifier was fed to a 7.45 khz sub-carrier oscillator which, in turn, modulated a 1680 Mhz transmitter.

The step generator is shown in Figure 24. The outputs of three flip flops are linearly added and amplified to produce a waveform as shown in Figure 25. The generator was changed from a sweep voltage to a staircase for a number of reasons:

1. Available transmitters at 1680 Mhz have poor modulation characteristics with more than one subcarrier. With a step voltage



NO.	DESCRIPTION	QTY.	UNIT
1	NOSE CONE	1	PC
2	NOSE CONE ATTACHMENT	1	PC
3	NOSE CONE ATTACHMENT	1	PC
4	NOSE CONE ATTACHMENT	1	PC
5	NOSE CONE ATTACHMENT	1	PC
6	NOSE CONE ATTACHMENT	1	PC
7	NOSE CONE ATTACHMENT	1	PC
8	NOSE CONE ATTACHMENT	1	PC
9	NOSE CONE ATTACHMENT	1	PC
10	NOSE CONE ATTACHMENT	1	PC
11	NOSE CONE ATTACHMENT	1	PC
12	NOSE CONE ATTACHMENT	1	PC
13	NOSE CONE ATTACHMENT	1	PC
14	NOSE CONE ATTACHMENT	1	PC
15	NOSE CONE ATTACHMENT	1	PC
16	NOSE CONE ATTACHMENT	1	PC
17	NOSE CONE ATTACHMENT	1	PC
18	NOSE CONE ATTACHMENT	1	PC
19	NOSE CONE ATTACHMENT	1	PC
20	NOSE CONE ATTACHMENT	1	PC
21	NOSE CONE ATTACHMENT	1	PC
22	NOSE CONE ATTACHMENT	1	PC
23	NOSE CONE ATTACHMENT	1	PC
24	NOSE CONE ATTACHMENT	1	PC
25	NOSE CONE ATTACHMENT	1	PC
26	NOSE CONE ATTACHMENT	1	PC
27	NOSE CONE ATTACHMENT	1	PC
28	NOSE CONE ATTACHMENT	1	PC

ARCAS PAYLOAD ASSEMBLY	
DATE	
BY	
CHKD BY	
APP'D BY	
REV.	

Fig. 19. Assembly drawing of Arcas payload.

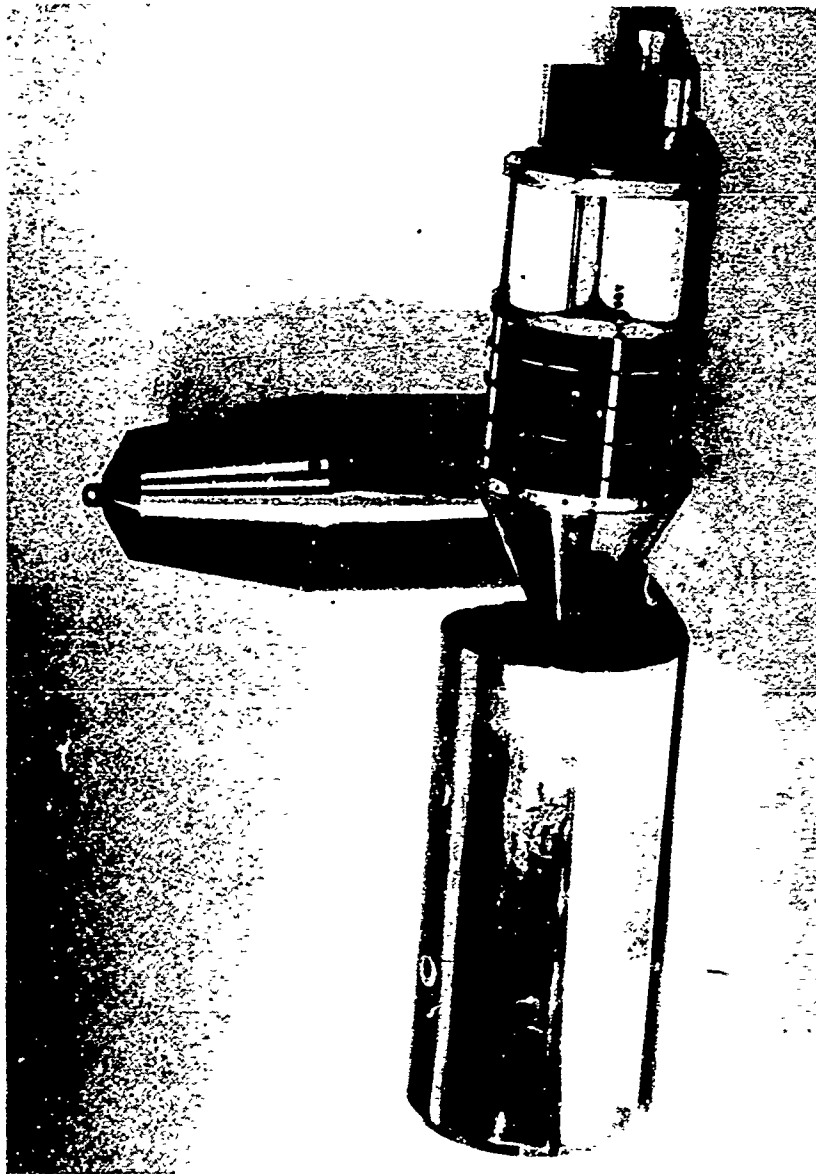


Fig. 20. Arcas Gardien condenser package.

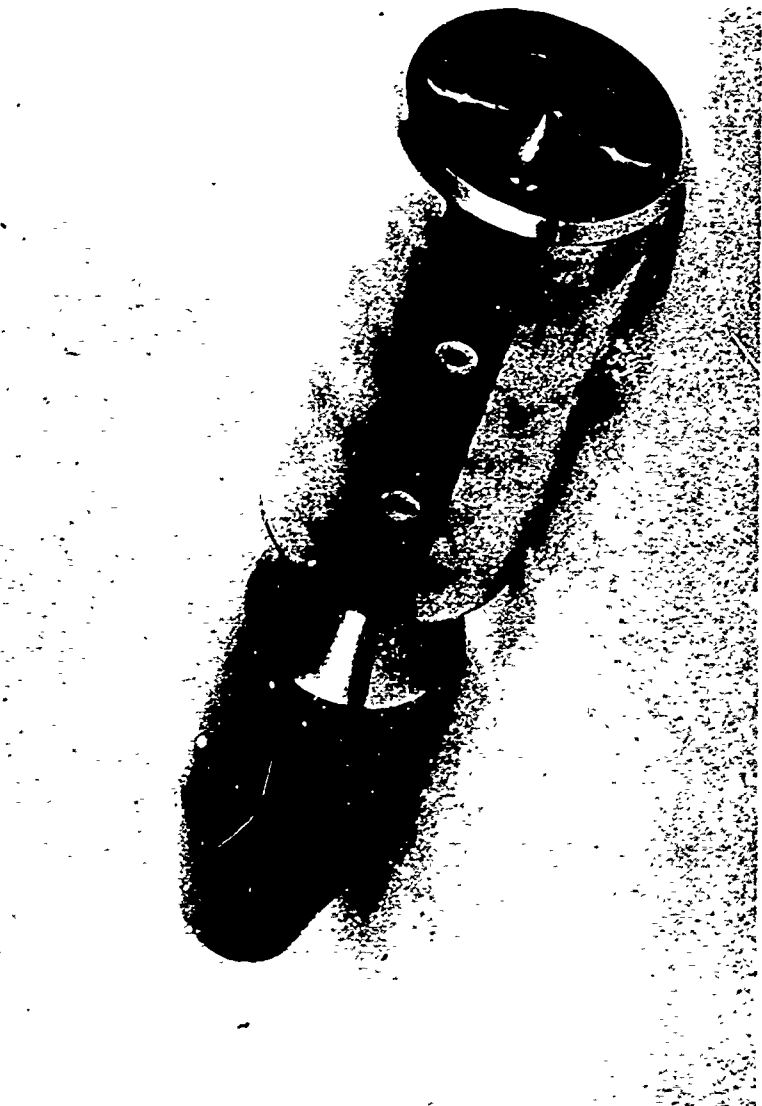


Fig. 21. Assembled Arcas Gerdien condenser.

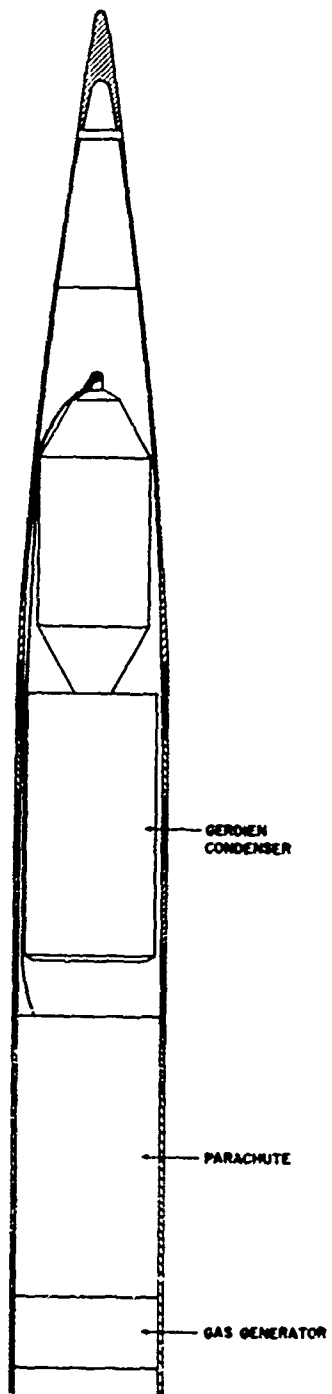
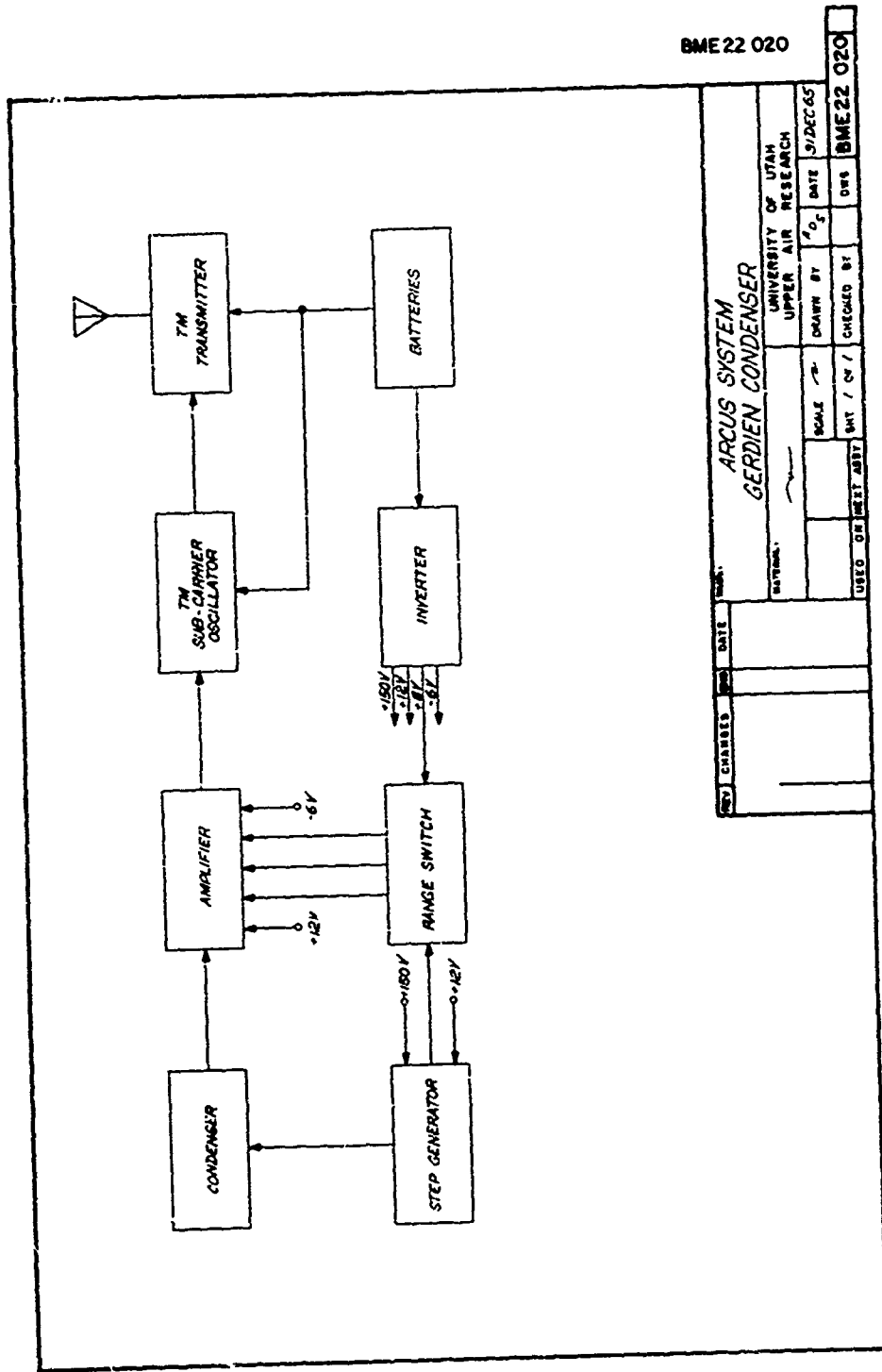


Fig. 22. Sketch of Arcas Gerdien condenser payload.



ARCUS SYSTEM GERDIEN CONDENSER	
UNIVERSITY OF UTAH UPPER AIR RESEARCH	DATE 31/DEC 65
SCALE	DRAWN BY
USED ON	CHECKED BY
OR	DWG
BME 22 020	

Fig. 23. Gerdien condenser block diagram (Arcas).

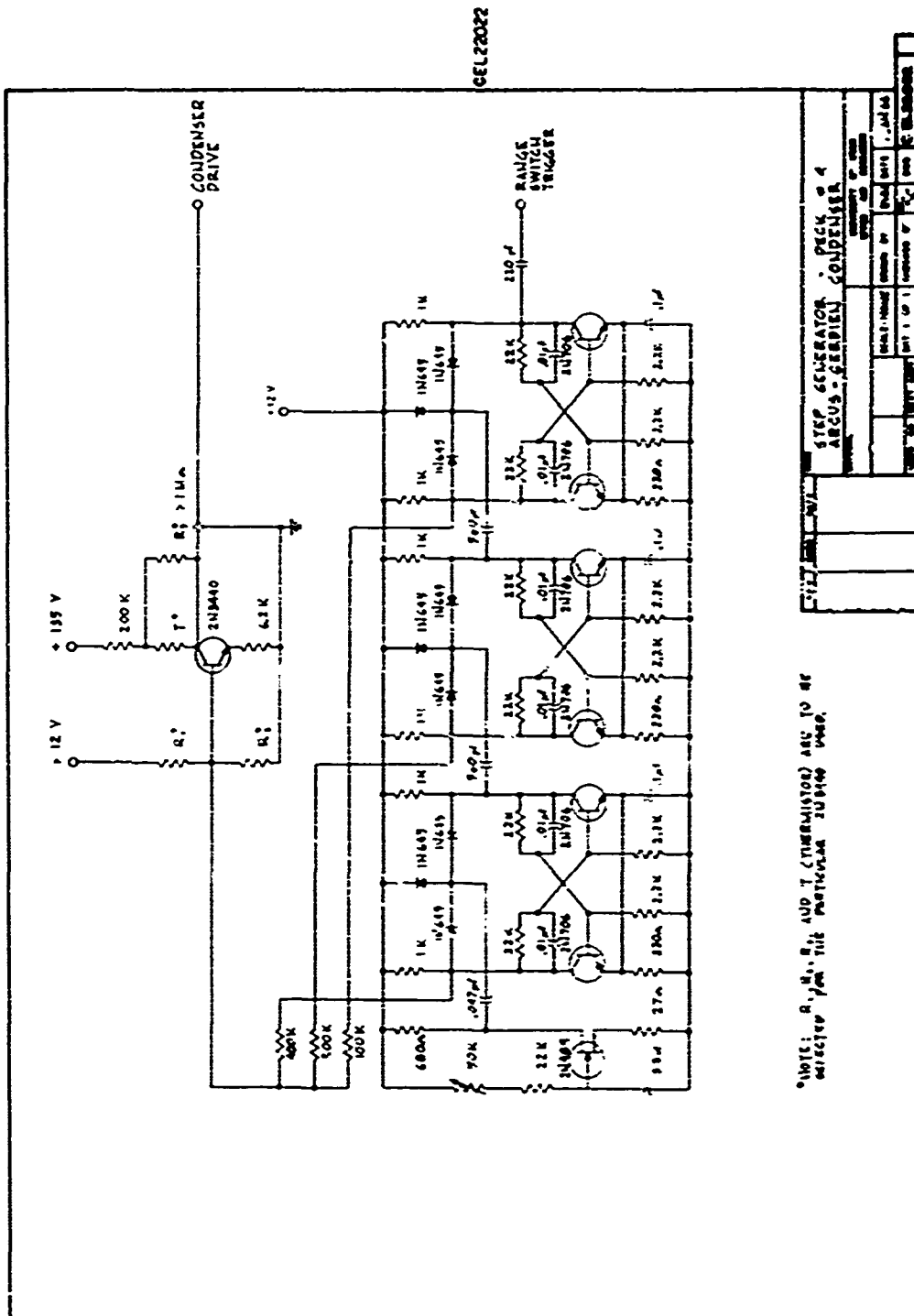


Fig. 24. Gardien condenser step generator (Arcas).

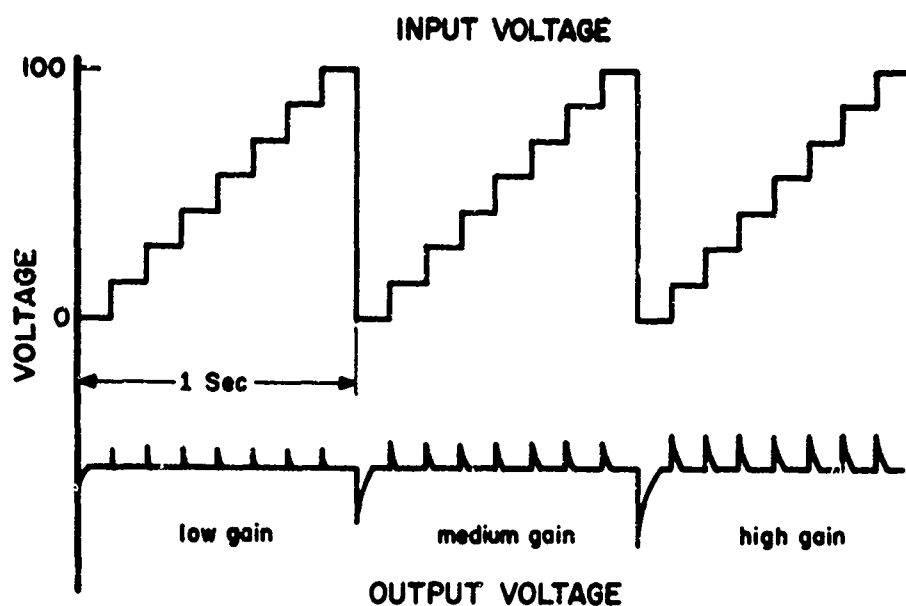


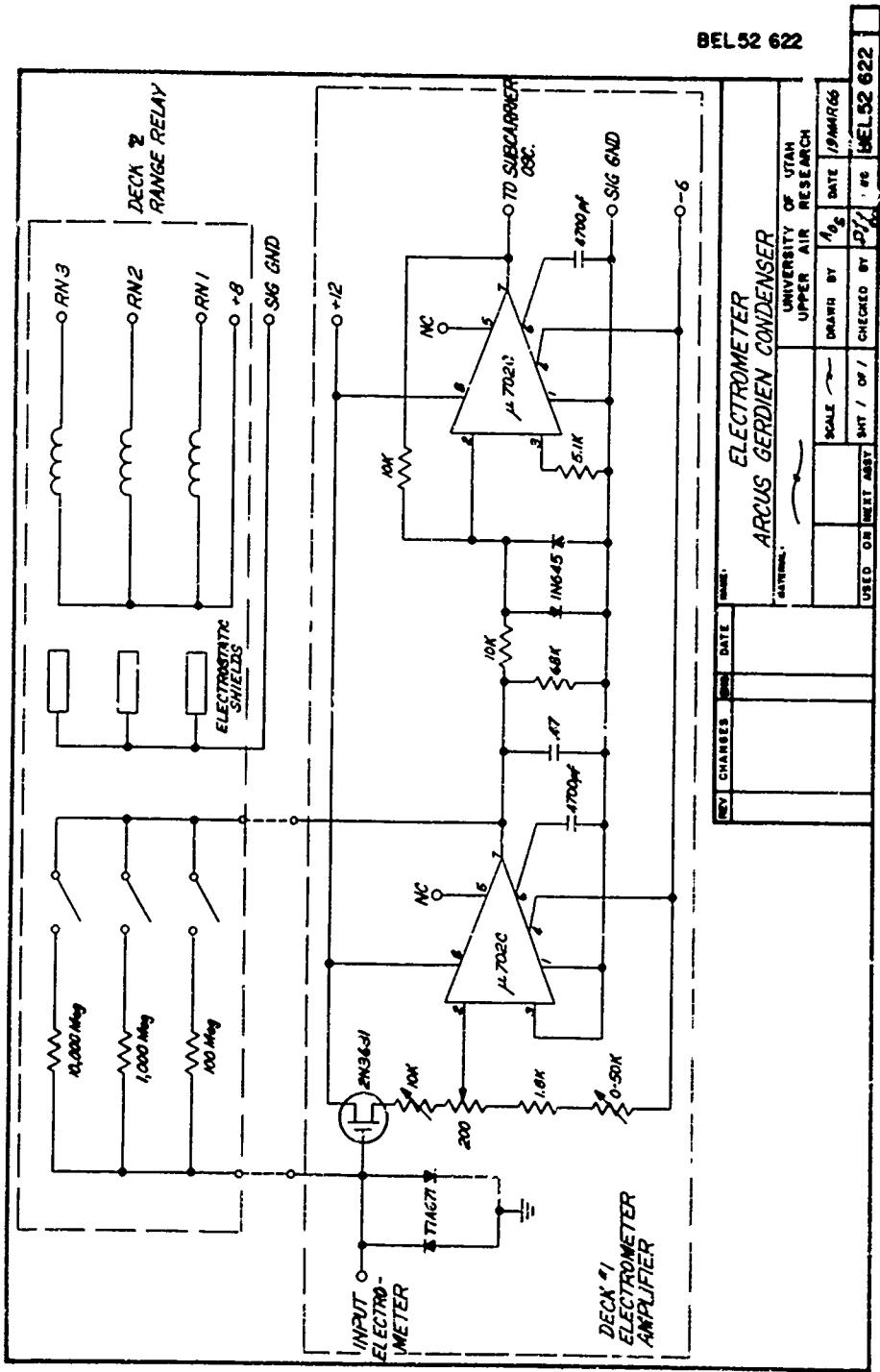
Fig. 25. Gerdien condenser stepped voltage waveform (Arcas).

the output of the amplifier appears as shown in Figure 25. The width of the negative spike varies depending on the gain range of the amplifier. Hence, the applied voltage and the gain range are known at any time without the use of a second subcarrier.

2. With a step input, the displacement current is dispatched rapidly, thereby eliminating the need of a negative generator for neutralizing the condenser capacitance.

The amplifier and the dc to dc converters, which are essentially the same as in the Black Brant, are shown in the schematics of Figures 26 through 28.

BEL 52 622



ARCUS GERDIEN CONDENSER
ELECTROMETER

UNIVERSITY OF UTAH
UPPER AIR RESEARCH

DRAWN BY: / / DATE: / / 1966

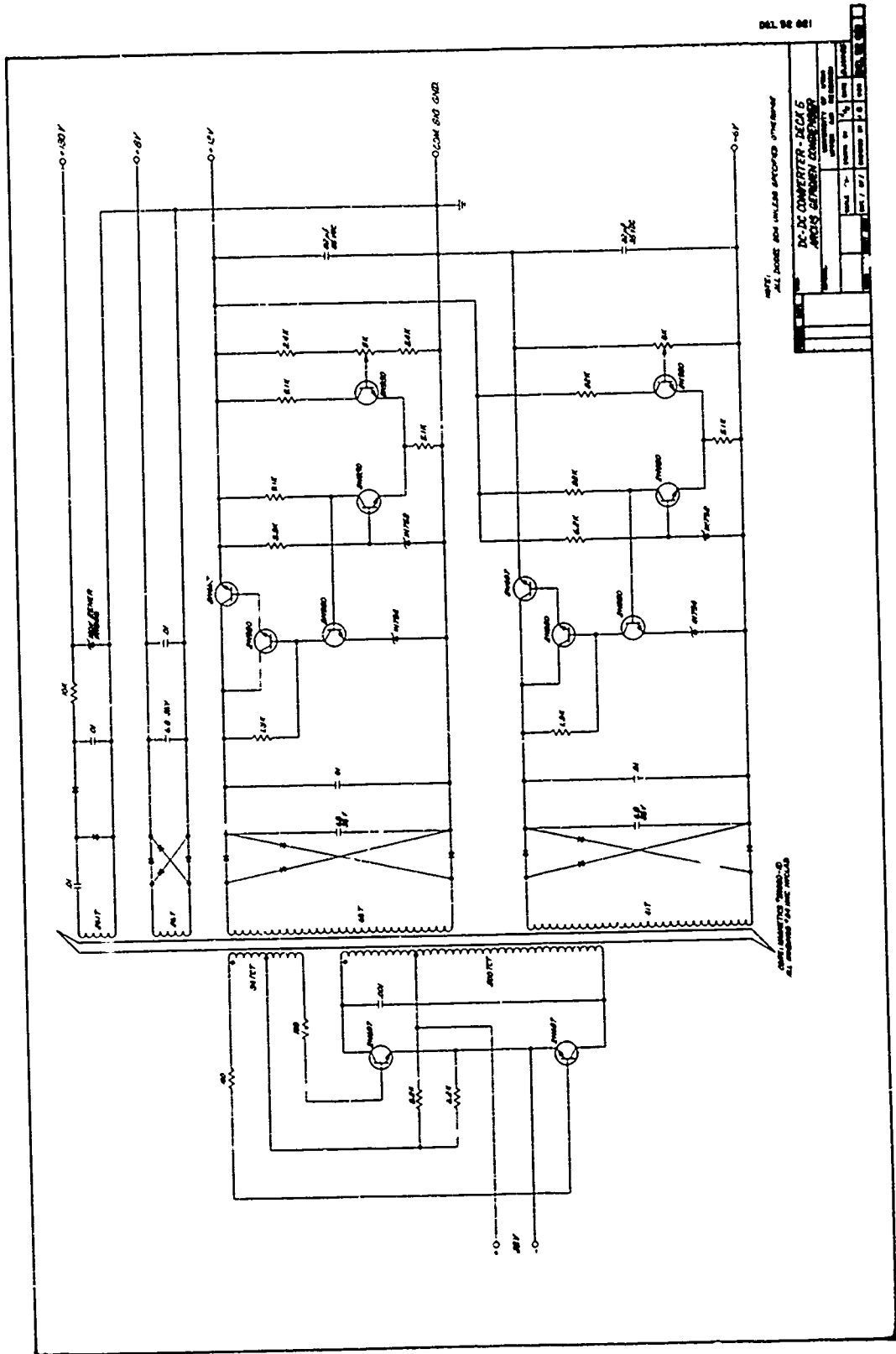
SCALE: / /

USED ON INSTR. ASST. / /

CHECKED BY: / /

BEL 52 622

Fig. 26. Gerdien condenser electrometer amplifier (Arcas).



FLIGHT PERFORMANCE

One Arcas payload was flown on 1 April 1966, at Churchill Research Range, Fort Churchill, Manitoba, Canada. The other Arcas and also the Black Brant payloads were flown at the same site on 28 September 1966.

Both Arcas rockets malfunctioned; the first one never reached altitude and radar track was lost on the second, indicating that the parachute was never ejected. The sweep voltages on the Black Brant rocket were gradually shorted out during the low altitude portion of the flight. The exact cause is not known; however, it has been suggested that the teflon insulator between the shield and the driven cylinder flowed due to the heat and caused the short.

A second set of Black Brant condensers have been built to the same dimensions with better insulation and are scheduled to fly during 1967.

CONCLUSIONS

With the present state of the art, it appears that the Gerdien condenser can be adapted to supersonic measurements. There may be basic limitations on measuring heavy negative ions due to the length and voltage requirement. Shock ionization appears to be no problem; however, there is some concern about the actual air flow through the condenser.

It is recommended that the actual air flow through the Gerdien condenser be determined by wind tunnel tests in the region of Mach 3. Wind tunnel tests at transonic speeds would have little bearing on the supersonic design; although information on the effective aperture and air flow in this region would be desirable for the parachute deployed payload.

The condenser design herein presented appears to be reasonable for initial investigation. However, it would be desirable to replace the support posts which hold the center electrode with slender fin-shaped supports to minimize the disturbance in the air flow. Although Pedersen has shown that measurements via a parachute return can be accomplished, it is highly desirable that additional tests be made in order to further develop the technique and better the understanding of the data.

After wind tunnel tests and with further improvements, the Gerdien condenser should prove to be an effective technique for measuring D-region conductivity.

REFERENCES

- Block, A.V., A.L. Kadis, and L.J. Smith, High altitude gun probes, *GCA Tech. Report 65-15-G*, Contract DA-19-020, AMC-0292 (R), GCA Corp., Bedford, 1965.
- Gerdien, H., Demonstration eines apparatus zur absoluten messung der elektrischen leitfähigkeit der luft, *Physikalische Zeitschrift*, 6, 800-801, 1905.
- Kidson, E., Atmospheric electricity observations on the first cruise of the "Carneigie", *Terrestrial Magnetism and Atmospheric Electricity*, 15, 83, 1910.
- Llepmann, H.W., and A. Roshko, *Elements of Gasdynamics*, pp. 406-431, John Wiley and Sons, Inc., New York, 1957.
- Murrow, H.N., Observations of parachute characteristics at altitudes above 100,000 feet by means of inflight photographs, paper presented at the Symposium on Parachute Technology and Evaluation, California, 1960.
- Narcisi, R.S., and A.D. Bailey, Mass spectrometric measurements of positive ions at altitudes from 64 to 112 kilometers, *J. Geophys. Res.*, 70, 3687-3700, 1965.
- Pedersen, A., Measurements of ion concentrations in the D-region of the ionosphere with a Gerdien condenser rocket probe, *Tellus*, XVII, 1, 1-45, 1965.
- Saha, M.N., and B.N. Srivastava, *A Treatise on Heat*, 4th edition, pp. 807-812, Hafner Publishing Co., New York, 1958.
- Swann, W.F.G., The theory of electrical dispersion into the free atmosphere with a discussion of the theory of the Gerdien conductivity apparatus and the theory of the collection of radioactive deposit by a charged conductor, *Terrestrial Magnetism*, 19, 81-92, 1914.
- Whitlock, C.H., and H.N. Murrow, Performance characteristics of a performed elliptical parachute at altitudes between 200,000 and 100,000 feet obtained by in-flight photography, *NASA Technical Note*, NASA TN D-2183, Langley Research Center, Virginia, 1964.

Unclassified

Security Classification

DOCUMENT CONTROL DATA - R & D		
<i>(Security classification of title, body of abstract and indexing annotation must be entered when the overall report is classified)</i>		
1. ORIGINATING ACTIVITY (Corporate author) Upper Air Research Laboratory University of Utah Salt Lake City, Utah 84112		2a. REPORT SECURITY CLASSIFICATION Unclassified
		2b. GROUP
3. REPORT TITLE THE DEVELOPMENT OF A GERDIEN CONDENSER FOR SOUNDING ROCKETS		
4. DESCRIPTIVE NOTES (Type of report and inclusive dates) Scientific. Interim.		
5. AUTHOR(S) (Print name, address initial, last name) David A. Burt		
6. REPORT DATE May 1967	7a. TOTAL NO. OF PAGES 51	7b. NO. OF REFS 10
8a. CONTRACT OR GRANT NO. AF 19(628)-4995 DASA WEB 07.007	9a. ORIGINATOR'S REPORT NUMBER UU-67-3	
8b. PROJECT, TASK, AND WORK UNIT NO. 5710, 7663-03, 76630301	9b. OTHER REPORT NUM (Any other numbers that may be assigned this report)	
8c. DOD ELEMENT 6164601D, 62405394	AFCRL-67-0343	
8d. DOD SUBELEMENT 681000		
10. DISTRIBUTION STATEMENT Distribution of this document is unlimited. It may be released to the Clearinghouse, Department of Commerce, for sale to the general public.		
11. SUPPLEMENTARY NOTES This research was sponsored in part by the Defense Atomic Support Agency, Wash., D.C.	12. SPONSORING MILITARY ACTIVITY Air Force Cambridge Research Laboratories (CRU) L.G. Hanscom Field Bedford, Massachusetts 01730	
13. ABSTRACT Measurements of D-region conductivity are of extreme importance in understanding the basic, normal atmospheric processes as well as for investigating special events associated with the D-region, i.e., auroral absorptions, polar cap absorptions (PCA) and sudden ionospheric disturbances (SID). This report discusses the theory and possibilities of adapting one type of conductivity probe, the Gerdien condenser for operation on sounding rockets at supersonic and subsonic velocities. Details are presented for two systems developed for making correlating measurements during simultaneous rocket flights. The first is designed for the Black Brant II rocket (supersonic flow); and the second, employing a parachute system, is designed for the Arcas rocket (subsonic flow). Authors		

DD FORM 1473

Unclassified

Security Classification

Unclassified
Security Classification

14. key words	LINK A		LINK B		LINK C	
	ROLE	WT	ROLE	WT	ROLE	WT
D-region conductivity						
Supersonic Gerdien condenser						
Ion measurements						

Unclassified
Security Classification